AD_____

Award Number: DAMD17-00-1-0071

TITLE: Genetics of Bone Mineralization and Morphology in Inbred Mice: Analysis of the HcB/Dem Recombinant Congenic Strains

PRINCIPAL INVESTIGATOR: Robert D. Blank, M.D., Ph.D.

CONTRACTING ORGANIZATION: The Hospital for Special Surgery
New York, New York 10021

REPORT DATE: April 2001

TYPE OF REPORT: Annual

PREPARED FOR: U.S. Army Medical Research and Materiel Command
Fort Detrick, Maryland 21702-5012

DISTRIBUTION STATEMENT: Approved for Public Release;
Distribution Unlimited

The views, opinions and/or findings contained in this report are those of the author(s) and should not be construed as an official Department of the Army position, policy or decision unless so designated by other documentation.

20020416 112

		Form Approved
# REPORT DOCUMENTATION PAGE		OMB No. 074-0188

Public reporting burden for this collection of information is estimated to average 1 hour per response, including the time for reviewing instructions, searching existing data sources, gathering and maintaining the data needed, and completing and reviewing this collection of information. Send comments regarding this burden estimate or any other aspect of this collection of information, including suggestions for reducing this burden to Washington Headquarters Services, Directorate for Information Operations and Reports, 1215 Jefferson Davis Highway, Suite 1204, Arlington, VA 22202-4302, and to the Office of Management and Budget, Paperwork Reduction Project (0704-0188), Washington, DC 20503

1. AGENCY USE ONLY (Leave blank)	2. REPORT DATE April 2001	3. REPORT TYPE AND DATES COVERED Annual (1 Apr 00 - 31 Mar 01)	
4. TITLE AND SUBTITLE Genetics of Bone Mineralization and Morphology in Inbred Mice: Analysis of the HcB/Dem Recombinant Congenic Strains			**5. FUNDING NUMBERS** DAMD17-00-1-0071
6. AUTHOR(S) Robert D. Blank, M.D., Ph.D.			
7. PERFORMING ORGANIZATION NAME(S) AND ADDRESS(ES) The Hospital for Special Surgery New York, New York 10021 E-Mail: rdb@medicine.wisc.edu			**8. PERFORMING ORGANIZATION REPORT NUMBER**
9. SPONSORING / MONITORING AGENCY NAME(S) AND ADDRESS(ES) U.S. Army Medical Research and Materiel Command Fort Detrick, Maryland 21702-5012			**10. SPONSORING / MONITORING AGENCY REPORT NUMBER**

11. SUPPLEMENTARY NOTES

12a. DISTRIBUTION / AVAILABILITY STATEMENT Approved for Public Release; Distribution Unlimited	12b. DISTRIBUTION CODE

13. ABSTRACT (Maximum 200 Words)

Susceptibility to osteoporotic fractures varies widely with genetic factors accounting for ~50% of this variation. Fracture risk is determined by peak bone mass and skeletal morphology achieved in young adulthood and the rate and extent of bone loss thereafter. This work will analyze the genetics of the first of these components through the use of recombinant congenic mice. We have demonstrated that the 27 HcB/Dem strains differ significantly in a variety of bone strength related phenotypes at 6 months of age. Further, preliminary mapping of genetic loci contributing to these phenotypes has been carried out. An intercross between HcB/13 and HcB/14 will allow more accurate mapping of a subset of these bone strength genes and investigation into pairwise epistatic interactions among loci. A cross examining $Cola2^{oim}/+$ heterozygotes will allow determination of whether segregating differential loci in this system map to the same chromosomal regions identified in the HcB/Dem studies. Further breeding will be performed to develop true congenic lines and refine the mapping of the candidate genes for their positional cloning. Identifying mouse chromosome regions that control peak bone mineralization and morphology will allow prediction of the corresponding human regions by synteny and facilitate human genetic studies of this problem.

14. SUBJECT TERMS osteoporosis, quantitative traits, epistasis, fractur risk, biomechanics, biomineralization			15. NUMBER OF PAGES 79
			16. PRICE CODE
17. SECURITY CLASSIFICATION OF REPORT Unclassified	**18. SECURITY CLASSIFICATION OF THIS PAGE** Unclassified	**19. SECURITY CLASSIFICATION OF ABSTRACT** Unclassified	**20. LIMITATION OF ABSTRACT** Unlimited

NSN 7540-01-280-5500

Standard Form 298 (Rev. 2-89)
Prescribed by ANSI Std. Z39-18
298-102

Table of Contents

Appendix 1: Yershov *et al.*, Bone Strength and Related Phenotypes in HcB/Dem Recombinant Congenic Mice (12 pp)

Appendix 2: IACUC Approval Letters (2 pp)

Appendix 3: Blank, Breaking Down Bone Strength: A Perspective (18 pp)

Appendix 4: Wurzburger *et al.*, Utility of GC Clamps in Mutation Detection By Denaturing High Performance Liquid Chromatography (34 pp)

Appendix 5: Wexler *et al.*, Bone Strength Variability in Mice Heterozygous for the $Cola2^{oim}$ Mutation (1 p)

Appendix 6: Camacho *et al.*, Emergence of Fracture-Resistant $Cola2^{oim/oim}$ Mice (1 p)

Appendix 7: Patani *et al.*, Use of Representational Difference Analysis to Identify Candidate RFLPs Linked to Modifiers of the Murine $Cola2^{oim/oim}$ Osteogenesis Imperfecta Phenotype (1 p)

Appendix 8: Goddard *et al.*, Geometry as a Heritable Determinant of Bone Strength (1 p)

INTRODUCTION

The broad purpose of this work is to understand the genetic basis of fracture risk. In order to accomplish this goal, we are working to detect and identify genes whose segregation alters bone biomechanical performance in young adult mice. Two crosses are being analyzed; the first is an intercross of recombinant congenic strains HcB/13 X HcB/14. These strains each carry 1/8 of their genomes from C57BL/10ScSnA and the remainder from C3H/DiSnA. HcB/13 are highly divergent in their bone properties, but only ~1/4 of the genome segregates in this cross, allowing analysis of epistatic interactions in a moderately sized cross. The second cross is between outbred B6C3/Fe-a/a-$Cola2^{oim/+}$ heterozygotes and B6C3/Fe-a/a F1 animals. The B6C3 background is closely related to the HcB/Dem system. In both cases, bones from 4 month animals will be phenotyped by 3-point bend testing, radiographic analysis, ash percentage, Fourier-transformed infrared spectroscopy, and histomorphometry. Histograms of the trait values will be used to select animals for use in linkage mapping, which will then be carried out using the QTL Cartographer software suite. Linkage mapping of distributed microsatellite markers will be supplemented by markers isolated through representational difference analysis of phenotypically extreme animals from each cross. QTLs identified in both crosses will be isolated through the generation of congenic lines by marker-assisted selection. The approach taken in this work expands on earlier investigations of bone genetics in that biomechanical performance is a primary endpoint and that pleiotropy testing of biomechanical outcomes and sub-phenotypes relates QTLs to specific components of bone strength.

BODY

Progress regarding item 2 of the statement of work has been on schedule, with task 2a nearly complete and tasks 2b and 2c initiated during year 1. Item 1 of the statement of work is behind schedule, however, and neither task 1a or 1b has yet been completed. Tardiness in accomplishing these tasks is due to delays arising from my moving from the Hospital for Special Surgery to the University of Wisconsin Medical School. Application for transfer of this award to the University of Wisconsin and a relinquishing statement from the Hospital for Special Surgery have been sent under separate cover. Below, progress in task 2 is summarized. This is followed by a brief discussion of the delay involved in accomplishing task 1.

Statement of Work item 2: Mapping background genes contributing to Cola2$^{oim/+}$ phenotypic variability

a. Phenotypic Analysis

Two hundred twenty five such animals were generated from 10 breeding pairs and sacrificed at 17 ± 1 weeks of age. Both males and females were studied by 3-point bend tests of the left humeri and several supporting phenotypes. Notably, none of the animals displayed evidence of spontaneous fracture by fine-focus radiographs obtained at sacrifice. The phenotypic analysis is summarized in **Table 1** below, with mean values $\pm$ standard deviations givenon the first line of each cell, with the minimum and maximum values given on the second line of each cell.

Table 1. Phenotypes of $Cola2^{oim/+}$ Heterozygotes

	Males (N = 119)	Females (N = 106)
Body Mass (g)	34.5 ± 4.9 18.1, 45.5	26.0 ± 3.8 18.5, 36.5
ML OD (mm)	1.46 ± 0.10 1.19, 1.72	1.36 ± 0.09 1.08, 1.72
AP OD (mm)	1.00 ± 0.08 0.82, 1.20	0.91 ± 0.07 0.76, 1.10
ML ID (mm)	0.69 ± 0.09 0.44, 0.92	0.66 ± 0.08 0.30, 0.84
AP ID (mm)	0.48 ± 0.07 0.30, 0.66	0.43 ± 0.06 0.28, 0.60
CSA (mm^2) (calculated)	0.89 ± 0.12 0.65, 1.23	0.75 ± 0.10 0.56, 1.12
I (mm^4) (calculated)	0.15 ± 0.04 0.07, 0.26	0.11 ± 0.03 0.05, 0.25
Failure Load (N)	8.42 ± 1.46 5.0, 11.8	7.05 ± 1.21 3.9, 10.0
Structural Stiffness (N/mm)	27.84 ± 6.11 11.9, 40.1	23.21 ± 5.09 12.5, 37.9
Failure Stress (MPa) (calculated)	75 ± 12 42, 111	80 ± 14 46, 108
Young's Modulus (MPa) (calculated)	1390 ± 310 790, 2350	1600 ± 310 780, 2610

ML = mediolateral, OD = outer diameter, AP = anteroposterior, ID = inner diameter, calculated indicates that values were calculated from directly measured values, as described in the original proposal's methods section.

The data demonstrate marked variation for all the measured phenotypes, generally greater values for males than females, and overlap between the values obtained in these animals and those obtained in the HcB/Dem animals summarized in the application for this award and reported in a manuscript (see appendix 1)(1). Also apparent from these data are greater diaphyseal diameters, CSAs, and Is and smaller failure loads, failure stresses, and moduli in the $oim/+$ heterozygotes relative to the HcB/Dem strains. In this, they are consistent with previously reported observations in this system (2) and in the $Mov-13$ system (3). Our phenotypic analyses of these animals are still incomplete, in that ash analysis is still in progress and bones from selected animals will be examined by histomorphometry.

As for the HcB/Dem data, we constructed a stepwise regression model for failure load as a function of other directly measured parameters. The model's R^2 = 0.664 and its equation is given by:

failure load = - 0.905 + 0.154 stiffness + 2.649 ML OD + 0.0325 mass

The results are quite similar to those obtained in the HcB/Dem studies, with structural stiffness contributing most of the model's explanatory power. Again as in the earlier study, forward and backward analyses yielded the same model. The effect of sex on failure load is completely accounted for by inclusion of body mass as an explanatory variable.

b. Representational difference analysis of extreme animals

The 225 animals described above have been rank-ordered for each of the traits analyzed thus far. We have purified genomic DNA from the top and bottom 10 animals of each sex and initiated representational difference analysis, as per statement of work items 2b and 2c.

Statement of Work Item 1: Intercross between HcB/13 and HcB/14

Progress on this item is approximately 6 months behind the original timetable for this award. This tardiness is attributable to disruptions in work attending my moving from The Hospital for Special Surgery to The University of Wisconsin. In September, 2000 I decided to accept a faculty position at the University of Wisconsin and began preparations to move my laboratory. Because of this decision, I delayed delivery of the HcB/13 and HcB/14 animals from Dr. Demant's laboratory in the Netherlands. I was seeking to minimize the animal issues by having them moved only once rather than twice. I moved in mid-November, 2000, having prepared a new animal protocol which was approved by the William Middleton Veterans' Hospital IACUC and, by reciprocity, The University of Wisconsin's IACUC (see appendix 2). I received the animals from the Netherlands in January, 2001. The F1 generation therefore had not reached the 17-week age of sacrifice by the end of year 1 of the award.

The Packard Multiprobe II purchased for this work was damaged in transit from New York to Madison, and repairs required over 1 month to complete. This delay, coupled with the time needed to train a new technician in the operation of this instrument delayed completion of the additional HcB/Dem genotyping.

Modification of Statement of Work in View of Research Performed to Date

Nothing learned in the fist year of this award suggests that the Statement of Work be modified in any significant way. The only modification requested is that the timetable be adjusted as a result of the late start to the breeding program. Please note that I anticipate that about half of the tardiness can be made up in year 2.

KEY RESEARCH ACCOMPLISHMENTS

- Demonstration that failure loads in $Cola2^{oim/+}$ heterozygous animals span a greater than 2-fold range of values
- Demonstration that sub-phenotypes of failure load in $Cola2^{oim/+}$ heterozygous animals also display marked variability
- Demonstration that long bone diaphyseal diameters in $Cola2^{oim/+}$ heterozygous animals are greater than in the HcB/Dem strains, consistent with the previous observation by Bonadio and colleagues that periosteal expansion in $Cola1^{Mov-13/+}$ mice occurs as an adaptation to defective type I collagen synthesis
- Emergence of attenuated bone fragility phenotypes in in $Cola2^{oim/oim}$ homozygous animals with inbreeding

REPORTABLE OUTCOMES

Manuscripts
The preliminary data included in the original application for this award are reported in a manuscript scheduled for publication in the June, 2001 issue of *The Journal of Bone and Mineral Research* (appendix 1) (1).

A perspective arising from a report by Beamer and associates (4) is also in press at *The Journal of Bone and Mineral Research* (appendix 3)(5).

A manuscript describing the use of GC-clamps as an aid to the design of denaturing high performance liquid chromatography has been submitted to *Clinical Chemistry*. The reviewers requested significant revisions of the manuscripts– primarily directed at shortening the report to approximately ¼ of its present length (appendix 4). While not a component of the approved Statement of Work, this work nevertheless could not have been accomplished without this award.

Abstracts
The $Cola2^{oim/+}$ phenotypic data summarized above were included in an abstract submitted to The American Society for Bone and Mineral Research 2000 annual meeting (appendix 5).

The *Cola2* investigations led to a serendipitous observation of attenuated phenotypes in partially inbred $Cola2^{oim/oim}$ homozygotes. This observation was presented in an abstract submitted to The American Society for Bone and Mineral Research 2000 annual meeting (appendix 6).

Representational difference analysis comparison of fully outbred $Cola2^{oim/oim}$ homozygotes and partially inbred $Cola2^{oim/oim}$ homozygotes is submitted as an abstract submitted to The American Society for Bone and Mineral Research 2001 annual meeting (appendix 7).

Geometry as a Heritable Determinant of Bone Strength is submitted as an abstract submitted to The American Society for Bone and Mineral Research 2001 annual meeting (appendix 8).

Patents and Licenses
None

Degrees Granted
None

Cell Lines and other Biological Reagents
None

Informatics Resources and Models
None

Other Funding

An application entitled "Phenotypic Attenuation in Murine Osteogenesis Imperfecta" was submitted to the NIH and assigned number AR48324. This application, with some modification, will also be submitted to the March of Dimes Birth Defects Foundation.

An application entitled "The Role of Genetic Background in Skeletal Adaptation to Increased and Decreased Loading" was submitted by Dr. M. C. H. van der Meulen to NASA and includes me as a consultant. This application relies on the divergence of HcB/13 and HcB/14 bone properties.

Employment and other Research Opportunities
None

CONCLUSIONS

Work in year 1 of this award is behind schedule with regard to Item 1 of the Statement of Work, but on schedule with regard to Item 2. Tardiness in accomplishing Item 1 is attributable to my move to the University of Wisconsin.

Results arising from Item 2 are consistent with the original study hypothesis that segregation of background genes contribute to phenotypic variability among $Cola2^{oim/+}$ heterozygotes. While no spontaneous fractures were observed in those animals, failure loads ranged from 3.9 to 11.8 N. While males and females differed, stepwise regression analysis modeling revealed that the apparent sex-related difference in phenotype could be accounted for by differences in body mass. Notably, both bone anatomy and calculated bone tissue components of failure load each demonstrated marked variability as well.

Genetic analysis of various other complex traits has demonstrated that mapping QTLs is in fact only 1 of several steps needed to understand the underlying biology. Another important step is to decompose the overall phenotype of interest into a series of sub-phenotypes whose inheritance is oligogenic, e.g. systemic lupus erythematosus (reviewed in (6)). This project is being conducted with this experience in mind; by mapping loci contributing to a series of related phenotypes in a single cross, pleiotropy testing allows phenotypic decomposition to be conducted simultaneously with linkage mapping. This argument is developed more fully in appendix 3 (5).

The bone community at large has also begun to appreciate the importance of bone phenotypes other than bone mineral density. The last year has witnessed an increasing number of publications and abstracts reporting on bone geometry, bone size, and the relation of these features to biomechanical performance (e.g. (7)). Ultimately, biomechanical performance under physiologic stresses is the single most important property of bone from the clinical perspective. Prediction of biomechanical performance is potentially important in the military setting in order to match personnel with duty assignments that they can perform effectively with minimal risk of injury.

REFERENCES

1.   Y. Yershov *et al.*, *J Bone Miner Res* **16**, (in press).
2.   J. Saban *et al.*, *Bone* **19**, 575-9 (1996).
3.   J. Bonadio *et al.*, *J Clin Invest* **92**, 1697-705. (1993).
4.   W. G. Beamer *et al.*, *J Bone Miner Res* **16**, (in press).
5.   R. D. Blank, *J Bone Miner Res* **16** (in press).
6.   E. K. Wakeland, A. E. Wandstrat, K. Liu, L. Morel, *Curr Opin Immunol* **11**, 701-7. (1999).
7.   S. S. Mehta, P. P. Antich, W. J. Landis, *Connect Tissue Res* **40**, 189-98. (1999); N. P. Camacho *et al.*, *J Bone Miner Res* **14**, 264-72. (1999); P. Augat *et al.*, *Med Eng Phys* **20**, 124-31. (1998); M. P. Akhter, D. M. Cullen, E. A. Pedersen, D. B. Kimmel, R. R. Recker, *Calcif Tissue Int* **63**, 442-9 (1998); M. Shimizu *et al.*, *Mamm Genome* **10**, 81-7 (1999).

Bone Strength and Related Traits in HcB/Dem Recombinant Congenic Mice

YEVGENIY YERSHOV,[1-3] TODD H. BALDINI,[1,2] SEAGRAM VILLAGOMEZ,[1,2,4] TODD YOUNG,[1,2,5] MELISSA L. MARTIN,[2,6] RICHARD S. BOCKMAN,[2,6] MARGARET G.E. PETERSON,[2] and ROBERT D. BLANK[2,6]

ABSTRACT

Fracture susceptibility depends jointly on bone mineral content (BMC), gross bone anatomy, and bone microarchitecture and quality. Overall, it has been estimated that 50–70% of bone strength is determined genetically. Because of the difficulty of performing studies of the genetics of bone strength in humans, we have used the HcB/Dem series of recombinant congenic (RC) mice to investigate this phenotype. We performed a comprehensive phenotypic analysis of the HcB/Dem strains including morphological analysis of long bones, measurement of ash percentage, and biomechanical testing. Body mass, ash percentage, and moment of inertia each correlated moderately but imperfectly with biomechanical performance. Several chromosome regions, on chromosomes 1, 2, 8, 10, 11, and 12, show sufficient evidence of linkage to warrant closer examination in further crosses. These studies support the view that mineral content, diaphyseal diameter, and additional nonmineral material properties contributing to overall bone strength are controlled by distinct sets of genes. Moreover, the mapping data are consistent with the existence of pleiotropic loci for bone strength–related phenotypes. These findings show the importance of factors other than mineral content in determining skeletal performance and that these factors can be dissected genetically. (J Bone Miner Res 2001;16:000–000)

Key words: skeleton, fractures, biomechanics, linkage genetics, quantitative trait

INTRODUCTION

FRACTURES OCCURRING as a consequence of skeletal fragility are an important health problem.[(1,2)] Yet, relatively little is known regarding the determination of bone strength. Most investigations have focused on bone mineral density (BMD), because this is a phenotype that is easily and reproducibly measured[(1)] and for which pharmacologic interventions are available.[(2)] However, although BMD possesses some predictive value with regard to human fracture risk, other risk factors have been identified, including past fracture history, maternal fracture history, visual acuity, height, level of physical activity, general health status, and use of steroids or anticonvulsants.[(3)] From epidemiological surveys, some of these additional risk factors appear to be comparable in importance with BMD but have not been studied in nearly as great detail.

Although the morbidity and mortality arising from skeletal fragility are suffered predominantly by the elderly, many aspects of bone strength are determined early in life.[(4)] Bone mass peaks at approximately age 30 years, with bone mineral loss occurring over the remainder of the life

---

[1]These authors contributed equally to this work.
[2]Mineralized Tissue Section, The Hospital for Special Surgery, New York, New York, USA.
[3]Present Address: State University of New York at Stony Brook Medical School, Stony Brook, New York, USA.
[4]Present Address: New York University School of Medicine, New York, New York, USA.
[5]Present Address: New York Medical College.
[6]Weill Medical College of Cornell University, New York, New York, USA.

Orig. Op.	OPERATOR:	Session	PROOF:	PE's:	AA's:	COMMENTS	ARTNO:
1st disk, 2nd ls	royerl	9	H3				0006290

2

cycle. Both peak bone mass achieved and rate at which bone loss occurs are complex traits, determined by interactions between genetic constitution and environmental factors. Overall, it has been estimated that 50–70% of bone strength is determined genetically.[3,5–14]

Because of the difficulty in performing studies of the genetics of bone strength in humans, we have used the HcB/Dem series of recombinant congenic (RC) mice to investigate this phenotype. The RC mice used in this report are inbred lines descended from third generation backcross brother-sister pairs in which strain C3H/DiSnA (C3H) was the background progenitor and C57BL/ScSnA (B10) was the donor progenitor.[15–17] Each of the 27 HcB/Dem strains carries an average of 12.5% B10 genome, but each has a different combination of donor and recipient strain alleles. The chromosome regions derived from each progenitor can be determined by genotyping for markers distributed throughout the genome. Because they are inbred, the results of mapping apply to all members of the strain and are cumulative. Phenotyping RC strains allows one to include multiple individuals as replicates, allowing generation of sample sizes that are sufficiently large to establish the presence of small differences between individual strains, just as is true of any inbred strain.

The experiments reported here were performed to achieve three objectives. First, we sought to describe the long bone properties of C3H, B10, and 24 of the HcB/Dem strains. Failure load, structural stiffness, failure stress, and modulus were determined through three-point bend tests of the animals' left humeri. Middiaphyseal inner diameter (ID) and outer diameter (OD) cross-sectional area (CSA), and moment of inertia (*I*) were determined through image analysis of radiographs. Ash percentage of femora from the same animals was determined gravimetrically. Body mass and body mass index (BMI) were determined by weighing and measuring animals at death. Second, these phenotypic data and the published HcB/Dem genotypic data[18,19] were used to perform quantitative trait locus (QTL) linkage mapping of the genes that contribute to the measured phenotypes. Third, we investigated the interrelationships among the various bone properties by developing multivariate regression models of failure load and by examining patterns of pleiotropy among the QTLs discovered by linkage analysis. The ability to define components of biomechanical performance and map them individually contributes to a deeper understanding of how genetic factors determine bone strength than would the study of any single parameter. This comprehensive approach allows simultaneous estimation of the degree to which individual parameters share common genetic determinants and the contribution of each identified genomic region to biomechanical performance.

MATERIALS AND METHODS

Mice

The HcB/Dem strains were established and are maintained at the Netherlands Cancer Institute. Briefly, the HcB/Dem mice are inbred strains derived from arbitrary pairs of N3 backcross animals.[15–17] The HcB/Dem strains have been genotyped at 130 marker loci distributed over each of the autosomes.[18,19] Because they are inbred, individuals from a single strain have the same genetic composition, except for new mutations and residual unfixed chromosome segments.[20,21] Less than 5% of the genome was unfixed at the time of genotyping; residual heterozygosity is expected to be reduced by half in each generation of inbreeding. The mice described in this report were provided by Dr. Peter Demant and maintained at the Hospital for Special Surgery until 6–7 months of age under 12 h light-dark cycling and fed irradiated PICO 5058 rodent chow and autoclaved tap water ad lib. Beamer and colleagues have reported that although mice continue to grow over the lifespan, peak bone mass is achieved at 4 months of age.[22] We examined strains HcB/1 through HcB/9, HcB11 through HcB/15, HcB/17, HcB/18, HcB/20 through HcB/23, HcB/25, HcB/26, HcB/28, and HcB/29. HcB/16 is extinct and HcB/27 is an unassigned number; so HcB/10, HcB/19, and HcB/24 were unexamined because these strains were unavailable at the time the experiments described here were performed. Between 4 and 10 animals of each strain were studied, yielding 179 HcB/Dem mice. Animals were allowed ad lib activity and were housed 1–5 animals/cage. Only females were studied, because inclusion of males would have introduced sex-dependent variability in the traits in addition to the strain-specific and environmental variability already encountered. At death, body mass and rostroanal length were measured. This work satisfied The Hospital for Special Surgery's requirements for the ethical use of laboratory research animals.

Ash percentage

Bone mineral fraction was calculated by comparison of dry, defatted bone weight to ash weight of homogenized tissue.[23,24] We chose to use entire bones rather than bones from which the epiphyses and marrow have been removed because the former technique is more reproducible in our hands. No ash data were obtained from the HcB/6 strain because of a laboratory accident.

Radiographic analysis

Image analysis of fine focus contact radiographs of dissected humeri was performed as described and used to calculate CSA and I.[24] Humeral length was defined as the distance along the diaphysis from the trochlea to the humeral head's most distant point. ODs and IDs were measured in orthogonal projections just distal to the deltoid tuberosity, perpendicular to the diaphyseal axis. CSA was calculated according to the elliptical approximation

$$CSA = \pi(ML\ OR * AP\ OR - ML\ IR * AP\ IR),$$

where OR is the outer radius and IR is the inner radius in either the mediolateral (ML) or anteroposterior (AP) projection. I also was calculated according to the elliptical approximation[25]

$$I = \pi/4[(ML\ OR)^3(AP\ OR - (ML\ IR)^3(AP\ IR)].$$

AQ1

Roberts,
AQ:3
NY

MTS
Systems,
Eden
Prairie,
MN
Instron,
Canton,
MA

AQ:5

Image analysis was performed with SigmaScan (Jandel Scientific) image analysis software. All radiographs included stepped aluminum densitometric phantoms. Radiographic images were digitized with a Kodak digital camera, with the photographic field including a length scale.

Biomechanical testing

Quasi-static three-point bend testing was performed on left humeri using posts designed and machined in-house with the MTS apparatus and Instron electronics as described.[26,27] Humeri were oriented with the deltoid tuberosity downward and the specimens were oriented with the central post adjacent to the distal end of the deltoid tuberosity. This orientation corresponds to the ML axis being parallel to the applied force. Posts were separated by 3.75 mm except for the B10 specimens, which were tested at a post separation of 3.0 mm.

Biomechanical data were analyzed following several important assumptions. First, we assumed that bone strength is determined entirely by the cortical bone in the middiaphysis. Second, we assumed that the humeral diaphysis is an ellipse with its major axis lying in the ML plane and its minor axis lying in the AP axis. Calculated biomechanical parameters were obtained according to the following standard formulas for three-point bending of ellipses[25]: stress $(\sigma; MPa) = FLc/4I$, where F is force, L, is length, and c is ML OR; strain $(\epsilon; mm/mm) = 12cd/liter^2$, where c is ML OR, d is displacement, and L is length; and Young's Modulus $(E; MPa) = (F/day)(L^3/48I)$.

Linkage analysis

Linkage mapping was carried out using the QTL cartographer software suite,[28,29] using sib-recombinant inbred as the cross type. The breeding scheme of RC mice is equivalent to that for recombinant inbred mice except for the fact that full-sib matings are started after the third backcross rather than the second filial generation. This breeding scheme results in multiple opportunities for recombination to occur before fixation of the genotype. Consequently, linkage relationships are weakened according to the relationship $R = 4r/(1 + 6r)$, where R is the observed fraction of recombinant genotypes and r is the single generation recombination fraction between a pair of loci.[20,21] Briefly, data were first analyzed for normality and those traits for which Fisher's cumulant test for normality[30] was significant at the 5% level were log-transformed (failure stress, modulus, body mass, and BMI) before further analysis. Transformed data were distributed normally by this criterion. Interval mapping was carried out to generate the final model.[31,32] A permutation test using 1000 simulated data sets was performed to estimate empirically significance levels.[33,34] Linkage maps were plotted with Gnuplot.[35] Linkage maps were generated for strain-averaged data.

Other statistical analysis

All values are shown as the mean ± SD. Continuous variables were analyzed by analysis of variance (ANOVA) f test. Phenotypes that were not distributed normally were
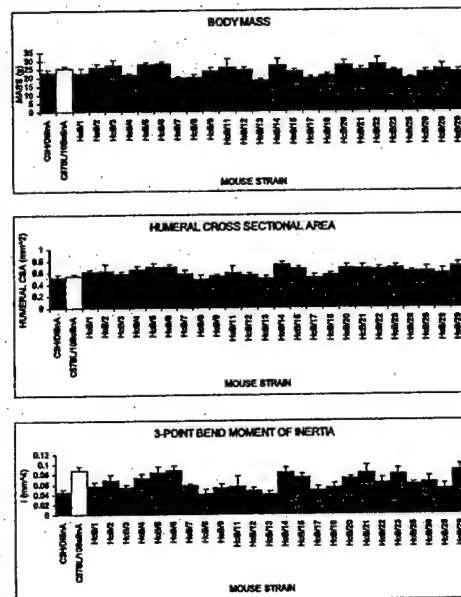

FIG. 1. Body masses, humeral CSAs, and humeral Is for the HcB/Dem strains. Each bar graph shows the average ±1 SD for C3H/DiSnA, C57BL/10ScSnA, and each of the HcB strains tested. Sample sizes range between 4 and 10 animals/strain.

log-transformed before analysis. In the specific case of BMI, the transform was log(1 + BMI). In general, the α-level was 0.05 with adjustment for multiple comparisons. We used linear regression with stepwise addition and backward elimination to generate the multivariate model for failure load as a function of the other parameters, using an initial inclusion criterion of $p < 0.047$ for adding parameters and a criterion of $p < 0.05$ for their retention.

RESULTS

Size and skeletal morphology

The body masses, humeral CSAs, and Is are shown in Fig. 1. The parental strains do not differ with respect to body mass or CSA, with C3H mice having a body mass of 23.2 ± 1.5 g and a CSA of 0.53 ± 0.03 mm^2 and B10 mice having a body mass of 25.4 ± 1.4 g and a CSA of 0.55 ± 0.04 mm^2. However, they differ markedly with respect to I (0.044 ± 0.005 mm^4 for C3H and 0.089 ± 0.007 mm^4 for B10). Although only I differs between the parental strains, each of these parameters varies markedly among the HcB/Dem strains. Minimum and maximum values for the various parameters and the corresponding strains are shown in Table 1. Also included in Table 1 are summary data for the diaphyseal diameters used to calculate CSA and I. The distribution of values among the HcB/Dem strains is con-

F1

T1

Orig. Op.	OPERATOR:	Session	PROOF:	PE's:	AA's:	COMMENTS	ARTNO:
1st disk, 2nd ls	royert	9					0006290

TABLE 1. PARENTAL PHENOTYPES AND PHENOTYPIC RANGES

| Trait	Parentals		All strains	
	C3H/DiSnA (C3H)	C57BL/ 10ScSnA (B10)	Minimum value and strain	Maximum value and strain
Body mass (g)	23.2 ± 1.5	25.4 ± 1.4	18.2 ± 0.5 HcB/13	27.9 ± 1.3 HcB/6
BMI (g/cm^2)	0.270 ± 0.014	0.295 ± 0.017	0.232 ± 0.010 HcB/25	0.311 ± 0.009 HcB/3
Humeral ML OD (mm)	1.06 ± 0.03	1.33 ± 0.04	1.02 ± 0.06 HcB/13	1.33 ± 0.04 B10
Humeral AP OD (mm)	0.83 ± 0.04	0.96 ± 0.04	0.81 ± 0.05 HcB/8	0.98 ± 0.02 HcB/14
Humeral ML ID (mm)	0.53 ± 0.05	0.89 ± 0.09	0.46 ± 0.06 HcB/22	0.89 ± 0.09 B10
Humeral AP ID (mm)	0.39 ± 0.03	0.65 ± 0.04	0.31 ± 0.04 HcB/3	0.65 ± 0.04 B10
Humeral CSA (mm^2)	0.53 ± 0.03	0.55 ± 0.04	0.49 ± 0.06 HcB/8	0.72 ± 0.05 HcB/14
Humeral I (mm^4)	0.044 ± .005	0.089 ± .007	0.040 ± .007 HcB/13	0.089 ± .007 B10
Femoral ash percentage	69.1 ± 1.1	64.2 ± 1.9	64.2 ± 1.9 B10	70.2 ± 1.5 HcB/23
Failure load (N)	7.4 ± 0.3	7.7 ± 1.4	6.1 ± 1.0 HcB/13	10.4 ± 1.2 HcB/14
Structural stiffness (N/mm)	17.9 ± 3.7	21.2 ± 12.9	17.2 ± 5.2 HcB/18	40.8 ± 8.5 HcB/14
Failure stress (MPa)	173 ± 14	87 ± 11	87 ± 11 B10	192 ± 36 HcB/8
Young's modulus (MPa)	3570 ± 1160	1130 ± 700	1130 ± 700 B10	5340 ± 880 HcB/26

A

B
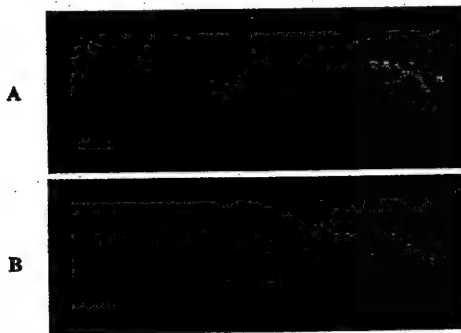
FIG. 2. Humeri of the parental strains. ML contact radiographs of (A) C3H/DiSnA and (B) C57BL/10ScSnA are shown.

sistent with segregation between the parental strains consistent with segregation between the parental strains contributing to each of these phenotypes. Body masses of the HcB/Dem strains ranged between 18.2 ± 0.5 g (HcB/13) and 27.9 ± 1.3 g (HcB/6). Most HcB/Dem strains had larger CSAs than the parental strains, ranging from a minimum of 0.49 ± 0.06 mm^2 (HcB/8) to a maximum of 0.72 ± 0.05 mm^2 (HcB/14).

The magnitude of the differences in CSA and I is shown in Fig. 2. Although CSA is equal between the parental strains, the source of their marked difference in I is apparent from this figure, which shows the striking dissimilarity of their diaphyseal diameters. Thus, although C3H mice have a thick diaphyseal cortex and a small diaphyseal diameter, B10 mice have the converse phenotype. This is reflected in I, which is proportional to the product of CSA and the square of the distance of that CSA from the bending axis for the three-point bending test. The divergence of CSA among the HcB/Dem strains arises as a result of dissociation of diaphyseal diameter from cortical bone thickness. HcB/14

has both a thick diaphyseal cortex and a large overall diameter, while HcB/8 is characterized by a thin cortex and a small overall diameter.

Biomechanical performance and ash analysis

We performed quasi-static three-point bending tests of the left humeri for each animal. In this test, the fracture is initiated in the plane of contact between the specimen and the central post of the apparatus. This protocol allows the central post to be placed at a recognizable anatomical site and measurements of the bone can be made at the same site. Results of these studies are summarized in Table 1 and Fig. 3. Failure load is one of the most basic measures of structural strength—the force needed to fracture the bone. The parental strains do not differ in this parameter, with C3H mice having a failure load of 7.4 ± 0.3 N and B10 mice having a failure load of 7.7 ± 1.4 N. Nevertheless, a wide range of failure loads was observed over the HcB/Dem strains, from HcB/13's value of 6.1 ± 1.0 N to HcB/14's value of 10.4 ± 1.2 N. A similar pattern is seen for structural stiffness as well, with C3H having a value of 17.9 ± 3.7 N/mm and B10 having a value of 21.2 ± 12.9 N/mm. The most divergent strains are HcB/18 (17.2 ± 5.2 N/mm) and HcB/14 (40.8 ± 8.5 N/mm).

It is useful to distinguish between structural and material properties in considering biomechanical testing data. Structural properties characterize the specimen as a whole, encompassing both its anatomy and its material. The structural properties are measured directly during the performance of the test. Material properties, in contrast, are calculated from the measured structural properties and the measured anatomical parameters. Failure stress is the material analogue to failure load and corrects for a specimen's CSA and diameter at the break point. In contrast to the data for failure load, the parental strains have widely divergent failure stresses, 173 ± 14 MPa for C3H and 87 ± 11 MPa for B10. B10's failure stress is the minimum for the strains studied and
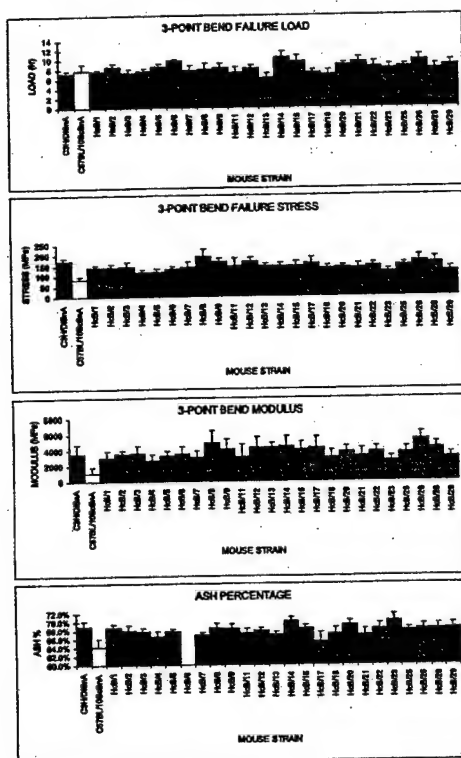
F3

F2

5

FIG. 3. Biomechanical performance of the HcB/Dem strains. Each bar graph shows the average ±1 SD for C3H/DiSnA, C57BL/10ScSnA, and each of the HcB strains tested. Sample sizes range between 4 and 10 animals/strain.

HcB/8's value of 192 ± 36 MPa is the maximum. Young's modulus is the material measure of stiffness; the parental strains' difference in failure stress is reflected by their moduli as well, with C3H having a modulus of 3570 ± 1160 MPa and B10 having a modulus of 1130 ± 700 MPa. B10 has the least stiff bone tissue observed in this study, whereas HcB/26, with a modulus of 5340 ± 880 MPa, has the stiffest bone tissue observed. These data show that both structural and material strength and stiffness vary widely among the HcB/Dem strains.

As a first step in characterizing the contribution of material properties to overall biomechanical performance, we performed ash analysis of femora from the same animals used for biomechanical testing. Ash percentage reflects the mineral content of the bone tissue and is the parameter most closely related to clinical measurements of BMD or bone mineral content (BMC). The results are summarized in Table 1 and Fig. 3 and show that C3H, with a value of 69.1 ± 1.1%, and B10, with a value of 64.2 ± 1.9%, differ markedly for this parameter. B10 has the minimum ash percentage of the strains studied and HcB/23, with a value

of 70.2 ± 1.5%, has the maximum ash percentage. Thus, substantial variations exist in the mineral content of bones from the HcB/Dem strains.

Contributions of the measured parameters to bone strength

Data presented in the previous section show that marked variations in animal size, anatomy as reflected by diaphyseal diameter and I, and BMC exist among the HcB/Dem strains and each of these are expected to contribute to differences in biomechanical performance among them. As an initial step in understanding the contribution of each of these parameters to biomechanical performance, we performed a simple correlation analysis of each of the parameters in a pairwise fashion, after log-transforming data for parameters with skewed distributions. Results of this analysis are summarized in Table 2.

We used these data to guide successive addition/elimination and elimination only stepwise regression analyses of failure load as a linear function of the other traits (Table 3). Such models express a single variable, in this case failure load, as a linear function of a subset of the other measured variables and an intercept given by the constant term of the equation. These other variables are included in the model only if they add to the model's explanatory power, as reflected by an increase in R^2. A perfect model has an $R^2 = 1.0$ and the R^2 value gives the fraction of the variation in failure load that is attributable to variation in the other traits.

In the first model, we used all other measured parameters as possible independent variables. This model found that over 90% of the failure load could be accounted for as a function of log(failure stress), CSA, and I. The model's $R^2 = 0.906$ and its equation is

$$failure\ load\ =\ -39.83\ +\ 18.63\ log(failure\ stress)$$
$$+\ 5.93\ CSA\ +\ 67.77\ I.$$

This model, although accounting for over 90% of the failure stress, is limited by the fact that failure stress is a function of load and I.

In the second model, we allowed only variables that were measured directly rather than calculated from measured quantities. This model had poorer predictive ability, accounting for nearly 57% of failure load. Its $R^2 = 0.568$ and its equation is given by

$$failure\ load\ =\ -13.48\ +\ 5.51\ log(structural\ stiffness)$$
$$+\ 0.11\ ash\%\ +\ 4.19\ log(body\ mass)\ +\ 1.97\ AP\ ID.$$

The majority of the explanatory power of this model came from the structural stiffness, which by itself explained 50% of the failure load. In both models, the same results were obtained by stepwise addition/elimination and elimination-only analyses.

Mapping of loci contributing to the phenotypes

Previously published genotypic data were used with the phenotypic analysis described previously to map loci contributing to each of the studied traits. The mapping data for

TABLE 2. CORRELATIONS AMONG BONE PARAMETERS

Parameters	Structure stiffness	Stress	Modulus	Ash %	I	CSA	ML OD	ML ID	AP OD	AP ID	Body mass	BMI
Load	0.714	0.236	0.272	0.505	0.707	0.726	0.655	0.275	0.442	0.294	0.454	0.236
	<0.001	0.002	<0.001	0.014	<0.001	<0.001	<0.001	<0.001	<0.001	<0.001	<0.001	0.002
Structure stiffness	—	NS	0.581	0.168	0.461	0.484	0.456	0.227	0.437	0.293	0.363	0.171
			<0.001	0.03	<0.001	<0.001	<0.001	0.003	<0.001	<0.001	<0.001	0.023
Stress		—	0.685	NS	−0.674	−0.641	−0.636	−0.331	−0.523	−0.303	−0.153	NS
			<0.001		<0.001	<0.001	<0.001	<0.001	<0.001	<0.001	0.046	
Modulus			—	NS	−0.388	−0.328	−0.412	−0.272	−0.211	NS	NS	NS
					<0.001	<0.001	<0.001	<0.001	0.006			
Ash %				—	NS	−0.449	NS	NS	0.157	NS	0.269	NS
						0.032			0.044		0.001	
I					—	0.893	0.959	0.566	0.716	0.462	0.461	0.192
						<0.001	<0.001	<0.001	<0.001	<0.001	<0.001	0.012
CSA						—	0.787	0.228	0.798	0.277	0.507	0.234
							<0.001	<0.001	<0.001	<0.001	<0.001	0.002
ML OD							—	0.649	0.533	0.372	0.454	0.222
								<0.001	<0.001	<0.001	<0.001	0.003
ML ID								—	0.289	0.267	NS	NS
									<0.001	<0.001		
AP OD									—	0.666	0.308	NS
										<0.001	<0.001	
AP ID										—	NS	NS
Body mass											—	0.786
												<0.001

Parameters were log-transformed before analysis. Significant correlation coefficients are shown on the top line and their associated p values are shown on the second line of each cell.

TABLE 3. STEPWISE REGRESSION MODELS OF FAILURE LOAD

Step	Parameter	p	Coefficient[a]	ΔR^2
	Model 1. All parameters included as potential independent variables			
1	Log(structural stiffness)	<0.001		0.432
2	ML OD	<0.001		0.0519
3	Log(stress)	<0.001	18.626	0.302
4	CSA	<0.001	5.927	0.113
5	I	<0.001	67.774	0.011
6	Remove log(structural stiffness)	0.126		−0.001
7	Remove ML OD	0.059		−0.002
	Model 2. Only directly measured parameters included as potential independent variables			
1	Log(structural stiffness)	<0.001	5.514	0.503
2	Log(body mass)	<0.001	4.192	0.040
3	Ash%	0.025	0.111	0.013
4	AP ID	0.035	1.973	0.012

[a] The coefficient is included only for those parameters retained in the final model.

selected chromosomes are summarized in Fig. 4. Mapping data for other traits (data not shown) reveal that LOD score graphs for all the diaphyseal diameters closely parallel each other. This also is true of CSA, I, failure stress, and modulus, which are calculated using the diaphyseal diameters. Because these parameters are codependent, only I is included in Fig. 4 along with the independently measured traits of failure load, structural stiffness, ash percentage, and body mass.

We performed a 1000-iteration permutation test to estimate experiment-wide significance levels for each trait as summarized in Table 4. As shown in Fig. 4, none of the strain-averaged QTL peaks achieved experiment-wide statistical significance,[36,37] regions on multiple chromosomes had LOD scores in excess of 1.7. An LOD ≥ 1 threshold is commonly used for exploratory genome scans of complex traits in a staged searching strategy.[36] However, given that we performed linkage mapping for five independently measured traits, it is appropriate to raise the exploratory threshold to the Bonferroni-corrected value of LOD ≥ 1.7.

On several chromosomes, LOD peaks for different traits map to the same genomic locations. Overlapping mapping
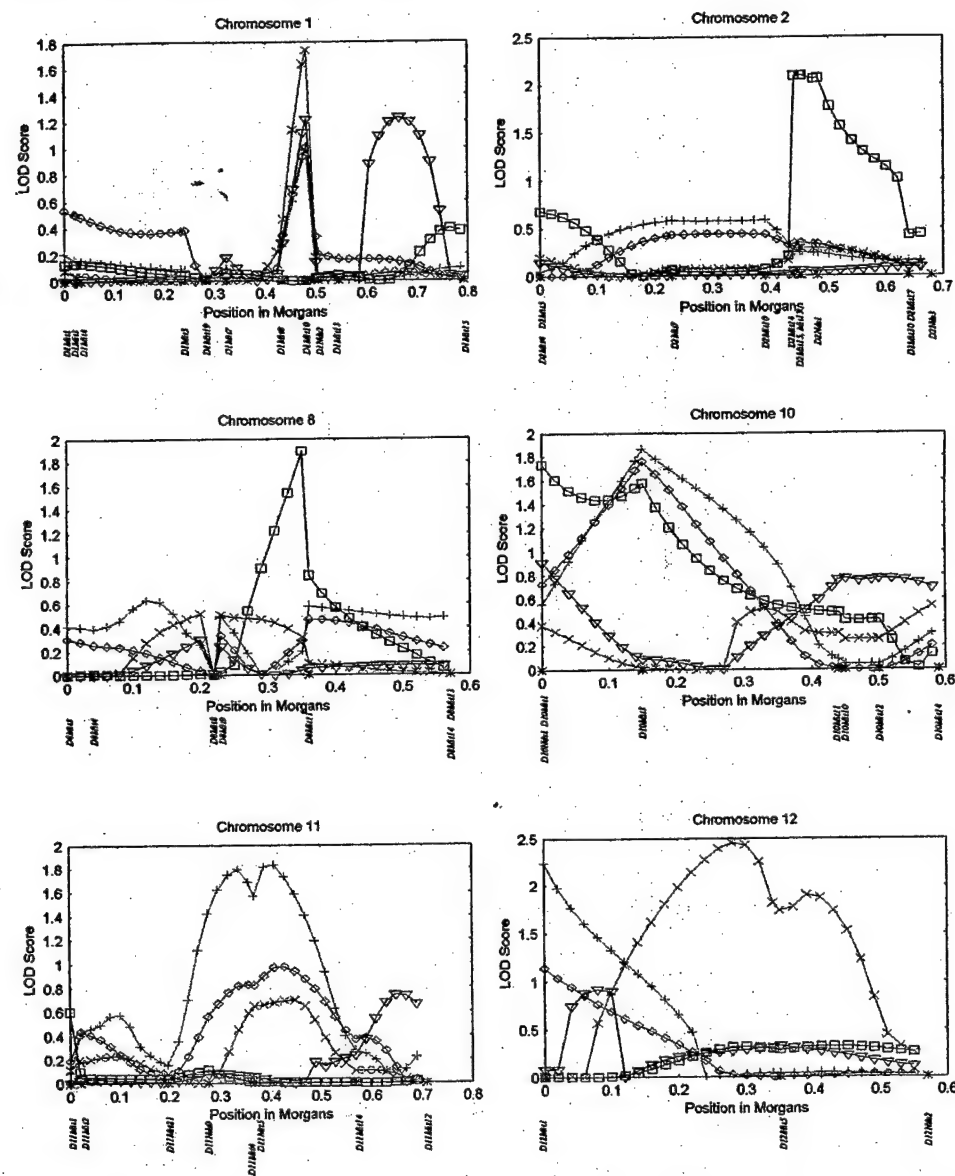
FIG. 4. Linkage maps for five traits. Linkage maps for failure load (red diamonds), structural stiffness (green + signs), ash percentage (blue squares), *I* (magenta X's), and body mass (navy triangles) are shown for each autosome in which the maximum LOD for any trait exceeded 1.0. The X dimension measures position in morgans (1 M = 100 cM) from the most centromeric marker. No "tails" flanking the outermost markers are included in the maps. The Y dimension measures LOD score. Marker positions are indicated below the *x* axis.

!

TABLE 4. EXPERIMENTAL-WIDE SIGNIFICANCE LEVELS

Significance level	Load	Structural stiffness	Ash%	I	Mass
0.01	3.45	3.22	2.96	3.47	3.52
0.025	3.01	3.03	2.77	3.22	3.17
0.05	2.71	2.79	2.55	2.92	2.88
0.10	2.45	2.44	2.41	2.62	2.59

assignments are consistent with the existence of pleiotropic (affecting multiple traits) QTLs at these locations. The degree of overlap among the mapping assignments is variable. Failure load and structural stiffness linkage maps are nearly parallel throughout the genome. A lesser degree of overlap is seen between failure load and *I*, and even less is observed between failure load and ash percentage. The linkage data suggest that there are distinct but overlapping sets of QTLs that contribute to each of the bone strength–related traits shown in the HcB/Dem system. This is well illustrated in comparing the maps of chromosomes 1 and 10 (Fig. 4). On chromosome 1, a peak centered at *D1Mit10* includes failure load, structural stiffness, *I*, and body mass, but not ash percentage. Conversely, the peak on chromosome 10 centered on *D10Mit3* includes failure load, structural stiffness, and ash percentage but not *I* or body mass.

DISCUSSION

This report presents bone phenotypes for 24 of the 27 HcB/Dem RC strains. These strains span nearly a 2-fold range of failure loads and vary widely for multiple related traits. Many phenotype pairs, even excluding those that are trivially related, display significant correlations. A multivariate linear regression model including only traits that were measured directly accounts for more than half the difference in failure load among the strains. The phenotypic data were used to generate the QTL maps for five independently measured traits in the HcB/Dem strains shown in Fig. 4.

The linkage maps reveal that potential QTLs for distinct traits sometimes colocalize to a single position in the genome, which we interpret as the presence of a single gene with pleiotropic effects (affecting multiple traits) at each multitrait LOD peak. An alternative explanation for colocalization is that distinct but closely linked QTLs are responsible for each of the phenotypes. Although the pleiotropy and multiple linked gene models cannot be distinguished by our data, the pleiotropy model is both more economical and consistent with present understanding of bone strength. Our data reveal coincident LOD peaks for distinct subsets of the traits at several positions in the genome. There is prior evidence relating these traits to failure load.[25,27,38–44] The existence of pleiotropic QTLs would provide a biological basis for the observed clinical correlations between body mass and bone strength. The biological importance of these putative pleiotropic loci is reinforced by the fact that they are based on very different, independently measured phenotypes. Mechanistically, pleiotropy most likely reflects the many developmental and biochemical steps separating the products of the putative

pleiotropic loci and the measured phenotypes. If one accepts the pleiotropy interpretation, it also is worth noting that colocalization of LOD peaks for multiple independent traits mitigates lack of statistical significance for linkage assignments. Permutation tests determine the frequency with which peaks of a given LOD threshold will occur anywhere in the genome by chance alone. Because there are many genomic locations where artifactual LOD peaks may occur, coincidence of peaks for multiple, independently measured traits can be interpreted more plausibly as representing biology rather than statistical accident. On this basis, we would predict that further experiments in this system are more likely to find significant QTLs on chromosomes 1, 10, and 11 than on chromosomes 2, 8, and 12.

In the linkage analysis, LOD scores may be increased because of epistasis between specific locus pairs. In previous work, Demant and colleagues showed large epistatic interactions between tumor susceptibility loci.[45,46] The small number of genotypes studied here will tend to magnify the contributions of individual loci, because main effects cannot be distinguished from interactions. These limitations of the data presented here can best be addressed by performing additional crosses; these are in progress.

Genetic differences are believed to account for a substantial portion of the variability in the bone strength of both mice and humans. In mice, Beamer and colleagues have measured volumetric BMD and cortical thickness by quantitative computed tomography (CT) scanning in a panel of 11 inbred mouse strains, noting that C57BL/6J and C3H/HeJ are the most extreme strains in their sample for these parameters.[22] These strains are related closely to the progenitors of the HcB/Dem RC strains. These investigators have begun to map volumetric BMD in crosses between C57BL/6J and CAST/EiJ[47] and between C57BL/6J and C3H/HeJ.[48] In these crosses, a highly significant QTL centered at *D1Mit15* falls in a region that may overlap with our LOD peak centered at *D1Mit10*. Two groups have studied the genetic basis of peak bone mass in the SAM/P6 senescence-accelerated, osteoporotic mouse. Shimizu and colleagues[49] used a midfemoral cortical thickness index as a measure of bone mass in a cross between SAMP6 and SAMP2, reporting a highly significant QTL on chromosome 11 between *D11Mit90 and D11Mit59* that may overlap our peak on that chromosome. Benes et al. have performed linkage mapping of areal BMD in crosses of SAMP6 with SAMR1 and AKR/J.[50] These workers also found a significant QTL in the corresponding chromosome 11 region. Klein and colleagues analyzed areal (i.e., projected) BMD in the B × D recombinant inbred strains as measured by dual-energy X-ray absorptiometry.[51] This study, like ours,

AQ:7

was exploratory in nature because of the limited number of genotypes examined. These related investigations have identified genomic regions that overlap partially with our results, providing independent evidence that LOD score peaks noted in the HcB/Dem system reflect true QTLs.

It is important to note two important differences between our experiments and the work performed by the other groups. First, although the phenotypes investigated are related, they are not the same and therefore may be under somewhat different genetic control. Second, the progenitors in each investigation are different. Consequently, in each system, a different set of loci and alleles segregates. These caveats are particularly important in relating the data presented here with other mapping studies. Colocalization of putative QTLs from different experiments, although providing evidence that a relevant gene is present, still requires caution if the phenotypic measures differ, as is true for chromosomes 1 and 11. Conversely, it is not surprising that some distinct loci contribute to bone strength in each experiment, given the diversity of traits and strains studied.

A human locus controlling bone mass (*HBM*) has been mapped to chromosome 11 q12–13[52] and there is evidence that this locus may account for variation in bone mass in a broader-based population as well.[53] The murine homologue to the human *HBM* locus is predicted to map to near the centromere of chromosome 19.

Thus far, mapping studies of bone properties have been heavily weighted toward radiographically determined mineral content as the phenotype. There are good reasons for this, most notably the existence of several well-characterized precise methods for measuring this parameter. However, as illustrated by the data presented here and consistent with clinical experience in humans, mineral content is only one among several factors contributing to overall bone strength and fracture risk.[39,40,43,54] Our observations also suggest that material properties of bone that were not investigated contribute to differences of failure stress and Young's modulus as well as failure load. These might include crystal size and morphology, degree of crystal perfection, degree of substitution of carbonate in the mineral, degree or pattern of collagen cross-linking, and differences in noncollagenous proteins. In this study, we have exploited the genetic homogeneity of inbred mice to allow biomechanical data to be used as a phenotype in a preliminary mapping study. The HcB/Dem RC strains each contain a distinct complement of B10 alleles on a background of the C3H genome. Both progenitors are "wild type," lacking mutations affecting skeletal structure, function, or development in an obvious fashion. Yet, the cumulative effects of allelic differences between these strains lead to quite dramatic differences in the cortical bone properties of adult mice.

Recently, increased attention has been focused on how anatomy affects bone strength in humans. Myers and colleagues[55] related load to fracture for cadaveric human forearms to BMD, BMC, CSA, and *I*. They found that both CSA and *I* were more predictive of biomechanical performance than either BMD or BMC measured by dual-energy X-ray absorptiometry, consistent with our phenotypic data. Several groups have suggested that a longer hip axis length (HAL) increases the risk of femoral neck fractures.[56–66] Bell and colleagues have reported cross-sectional data suggesting that loss of cortical bone mass in the anteroinferior-

posterosuperior axis of the femoral neck increases the risk of hip fracture.[67] They hypothesize that formation of "giant" Haversian canals in the femoral neck contributes to the specific loss of cortical bone mass.[68] Duan and colleagues assessed the contributions of reduced bone size and reduced volumetric BMD to vertebral fracture risk.[69] These investigators found in a cross-sectional sample that both contributed to fracture risk and that reduced vertebral body size accounted for 16% of the areal BMD deficit of fracture patients relative to controls. This bone size effect accounts for the apparent discrepancy between the work of Beamer and colleagues, who find C57BL/6J to be a low BMD strain, and that of Klein and colleagues, who find C57BL/6J to be the high BMD progenitor in the B × D recombinant inbred system. The Beamer group follows volumetric BMD whereas the Klein group follows areal BMD. Like C57BL/10ScSnA, the progenitor of the HcB/Dem RC series, C57BL/6J is characterized by a large diaphyseal diameter,[70] resulting in a bone volume–dependent increase in areal BMD. As in different strains of mice, humans display ethnic differences in bone volume[9,10,61,71–74] and bone size is a highly heritable trait.[3,5–8,11–14,75] Areal BMD's better performance in predicting fracture risk compared with volumetric BMD thus is seen to be the result of its inherently compound nature—it includes a measure of bone mineralization and superimposes an anatomic factor that reflects *I*.[73,76–81] Mapping QTLs that allow resolution of the anatomic and material aspects of bone strength therefore is a notable step toward unraveling the complexities of fracture risk.

Work to date has made it apparent that family relationships among genes have been conserved over evolution. One practical result of these findings is that genes' functions are similar in humans to their functions in model organisms. Moreover, we have learned that the organization of chromosome structure in these two species is highly conserved, with the preservation of so-called syntenies, or groups of physically linked genes that have remained together over the course of evolution. Only about 200 major chromosome rearrangements are thought to have occurred since the human and murine lineages diverged.[82–85] Therefore, a second practical consequence of the genome project's progress is that genetic mapping data from the mouse can be used to predict the locations of corresponding human genes. The existence of conserved synteny relationships will allow testing of the roles of genetic loci identified in the mouse in human populations.

The data presented previously are limited in several important ways. First, sample sizes are relatively small and are limited to 6-month-old female mice. Beamer and colleagues have shown that bone mass in mice does not remain constant throughout adulthood and that change in BMC follows different time courses in different strains.[22] Loss of bone mass during aging also has been established by the SAMP6 mouse, which develops osteoporosis as it ages.[86] Our data do not address any aspect of bone turnover over an individual's lifetime.

Second, there are important differences in bone metabolism between mice and humans. The mouse skeleton undergoes virtually no osteonal remodeling,[87] whereas such remodeling is a central feature of human bone. Although mice grow primarily during the first 4 months of life, their

epiphyses remain open throughout their lives. The murine estrous cycle is quite dissimilar to human menses and mice do not undergo menopause in midlife. Each of these differences limits the applicability of the findings reported here to human bone properties.

Third, important limitations accompany the choice of the HcB/Dem system. Only 24 strains were examined, limiting the power of the linkage study to an exploratory level. Mapping was performed with strain-averaged data, obscuring intrastrain variability and weighting the individuals from the strains with the smallest sample sizes most heavily. Genotypic data for the HcB/Dem strains only include approximately 130 markers and their genotypes include some relatively large untyped segments.[18,19] The RC breeding scheme aggravates the impact of gaps in the HcB/Dem strain distribution pattern. There are multiple opportunities for crossing over to occur during the inbreeding process, so that the extent of the genome spanned by each marker in RC lines is only approximately one-fourth that spanned by markers in a single-generation experiment.[20,21,88] There are likely to be additional small, unidentified differential segments between the two parental strains. Moreover, there may be segregating QTLs that contribute to the phenotypes examined that this experiment was unable to detect. Incorporation of additional markers to the HcB/Dem strain distribution pattern will allow this issue to be addressed.

Fourth, although biomechanical tests are more closely related to fracture risk than is BMC, the fractures generated in these tests are still artifactual with regard to fracture site and fracture mechanism. Three-point bending of the mouse humerus assesses cortical bone strength, because the site is virtually devoid of trabecular bone. The stresses that lead to human fragility fractures and hip fractures in particular probably differ from the fractures generated in our biomechanical tests in important ways.

Fifth, not all the phenotypes studied are of equivalent status. Failure load, structural stiffness, body mass, BMI, ash percentage, and the various diameters are measured directly. Failure stress, modulus, CSA, and I, in contrast, are calculated from the directly measured phenotypes. Although all measurements are subject to potential errors, only the calculated parameters are subject to compounded errors.

Sixth, the LOD scores of potential QTLs are systematically overestimated as discussed previously, primarily as a consequence of the small number of independent genotypes examined. This means that QTL mapping assignments based on either recombinant inbred or RC strain data must be confirmed in an independent breeding experiment. This limitation applies equally to the data presented here and those presented by Klein and coworkers.[51]

These limitations notwithstanding, the experiments reported here are a comprehensive analysis of the biomechanical properties of humeri and of their structural, material underpinnings and a preliminary investigation of their genetic basis in the HcB/Dem RC system. The virtue of combining QTL mapping with comprehensive phenotypic analysis is that insight is gained not only regarding the chromosomal locations of the genes contributing to bone strength, but also regarding the mechanisms by which strength is achieved.

REFERENCES

1. Kleerekoper M, Nelson DA 1997 Which bone density measurement? J Bone Miner Res 12:712–714.
2. Eastell R 1998 Treatment of postmenopausal osteoporosis. N Engl J Med 338:736–746.
3. Lutz J 1986 Bone mineral, serum calcium, and dietary intakes of mother/daughter pairs. Am J Clin Nutr 44:99–106.
4. Newton-John HF, Morgan DB 1968 Osteoporosis: Disease or senescence. Lancet 1:232–233.
5. Smith DM, Nance WE, Kang KW, Christian JC, Johnston CC Jr 1973 Genetic factors in determining bone mass. J Clin Invest 52:2800–2808.
6. Sowers MR, Burns TL, Wallace RB 1986 Familial resemblance of bone mass in adult women. Genet Epidemiol 3:85–93.
7. Pokock NA, Eisman JA, Hopper JL, Yeates MG, Sambrook PN, Ebert S 1987 Genetic determinants of bone mass in adults. J Clin Invest 80:706–710.
8. Dequeker J, Nijs J, Verstraeten A, Geusens P, Gevers G 1987 Genetic determinants of bone mineral content at the spine and radius: A twin study. Bone 8:207–209.
9. Liel Y, Edwards J, Spicer KM, Gordon L, Bell NH 1988 The effects of race and body habitus on bone mineral density of the radius, hip, and spine in premenopausal women. J Clin Endocrinol Metab 66:1247–1250.
10. Pollitzer WS, Anderson JJB 1989 Ethnic and genetic differences in bone mass: A review with a hereditary vs. environmental perspective. Am J Clin Nutr 50:1244–1259.
11. Christian JC, Yu P-L, Slemenda CW, Johnston CC Jr 1989 Heritability of bone mass: A longitudinal study in aging male twins. Am J Hum Genet 44:429–433.
12. Seeman E, Hopper JL, Bach LA, Cooper ME, Parkinson E, McKay J, Jerums G 1989 Reduced bone mass in daughters of women with osteoporosis. N Engl J Med 320:554–558.
13. Lutz J, Tesar R 1990 Mother-daughter pairs: Spinal and femoral bone densities and dietary intakes. Am J Clin Nutr 52:872–877.
14. Seeman E, Tsalamandris C, Formica C, Hopper JL, McKay J 1994 Reduced femoral neck bone density in the daughters of women with hip fractures: The role of low peak bone density in the pathogenesis of osteoporosis. J Bone Miner Res 9:739–743.
15. Demant P, Hart AA 1986 Recombinant congenic strains—a new tool for analyzing genetic traits determined by more than one gene. Immunogenetics 24:416–422.
16. Moen CJ, van der Valk MA, Snoek M, van Zutphen BF, von Deimling O, Hart AA, Demant P 1991 The recombinant con-

genic strains—a novel genetic tool applied to the study of colon tumor development in the mouse. Mamm Genome 1:217–227.

17. van Zutphen LF, Den Bieman M, Lankhorst A, Demant P 1991 Segregation of genes from donor strain during the production of recombinant congenic strains. Lab Anim 25:193–197.

18. Groot PC, Moen CJ, Dietrich W, Stoye JP, Lander ES, Demant P 1992 The recombinant congenic strains for analysis of multigenic traits: Genetic composition. FASEB J 6:2826–2835.

19. Stassen AP, Groot PC, Eppig JT, Demant P 1996 Genetic composition of the recombinant congenic strains. Mamm Genome 7:55–58.

20. Taylor BA 1978 Recombinant inbred strains: Use in gene mapping. In: Morse HC (ed.) Origins of Inbred Mice. Academic Press, New York, NY, USA, pp. 423–438.

21. Bailey DW 1981 Recombinant inbred strains and bilineal congenic strains. In: Foster HL, Small JD, Fox JG (eds.) The Mouse in Biomedical Research. Academic Press, New York, NY USA, pp. 223–239.

22. Beamer W, Donahue L, Rosen C, Baylink D 1996 Genetic variability in adult bone density among inbred strains of mice. Bone 18:397–403.

23. Donnelly R, Bockman R, Di Carlo E, Betts F, Boskey A 1993 The effect of gallium nitrate on healing of vitamin D- and phosphate-deficient rickets in the immature rat. Calcif Tissue Int 53:400–410.

24. Camacho NP, Rimnac CM, Meyer RAJ, Doty S, Boskey AL 1995 Effect of abnormal mineralization on the mechanical behavior of X-linked hypophosphatemic mice femora. Bone 17:271–278.

25. Turner CH, Burr DB 1993 Basic biomechanical measurements of bone: A tutorial. Bone 14:595–608.

26. Simske SJ, Luttges MW, Wachtel H 1990 Age Dependent Development of Osteopenia in the Long Bones of Tail-Suspended Mice ISA, vol. 90–014, pp. 87–94.

27. Ferretti JL, Spiaggi EP, Capozza R, Cointry G, Zanchetta JR 1992 Interrelationships between geometric and mechanical properties of long bones from three rodent species with very different biomass: Phylogenetic implications. J Bone Miner Res 7:S433–S435.

28. Basten CJ, Weir BS, Zeng Z-B 1994 Zmap—a QTL cartographer. In: Smith C, Gavora JS, Benkel B, Chesnais J, Fairfull W, Gibson JP, Kennedy BW, Burnside EB (eds.) Fifth World Conference on Genetics Applied to Livestock Production: Computing Strategies and Software, vol. 22, Guelph, Ontario, Canada, pp. 65–66.

29. Basten CJ, Weir BS, Zeng Z-B 1999 QTL cartographer, 1.13 ed. North Carolina State University, Raleigh, NC.

30. Kanji GK 1993 100 Statistical Tests. SAGE Publications, London, UK, pp. 42–44.

31. Lander ES, Green P, Abrahamson J, Barlow A, Daly MJ, Lincoln SE, Newburg L 1987 MAPMAKER: An interactive computer package for constructing primary genetic linkage maps of experimental and natural populations. Genomics 1:174–181.

32. Lander ES, Botstein D 1989 Mapping Mendelian factors underlying quantitative traits using RFLP linkage maps. Genetics 121:185–199.

33. Churchill GA, Doerge RW 1994 Empirical threshold values for quantitative trait mapping. Genetics 138:963–971.

34. Doerge RW, Churchill GA 1996 Permutation tests for multiple loci affecting a quantitative character. Genetics 142:285–294.

35. Williams T, Kelley C, Lang J, Kotz D, Campbell J, Elber G 1986–1993 Gnuplot, 3.0 ed.

36. Lander E, Schork N 1994 Genetic dissection of complex traits. Science 265:2038–2048.

37. Lander E, Kruglyak L 1995 Genetic dissection of complex traits: Guidelines for interpreting and reporting linkage results. Nat Genet 11:241–247.

38. Hayes W 1986 Basic Biomechanics of the Skeleton Current Concepts of Bone Fragility. Springer-Verlag, Heidelberg, Germany, pp. 3–18.

39. Cummings SR, Nevitt MC, Browner WS, Stone K, Fox KM, Ensrud KE, Cauley J, Black D, Vogt TM 1995 Risk factors for hip fracture in white women. Study of Osteoporotic Fractures Research Group. N Engl J Med 332:767–773.

40. Cummings SR 1996 Treatable and untreatable risk factors for hip fracture. Bone 18:165S–167S.

41. Nguyen TV, Eisman JA, Kelly PJ, Sambrook PN 1996 Risk factors for osteoporotic fractures in elderly men. Am J Epidemiol 144:255–263.

42. Ross PD, Davis JW, Epstein RS, Wasnich RD 1991 Pre-existing fractures and bone mass predict vertebral fracture incidence in women. Ann Intern Med 114:919–923.

43. Ross PD, Davis JW, Wasnich RD 1993 Bone mass and beyond: Risk factors for fractures. Calcif Tissue Int 53(Suppl 1):S134–S138.

44. Wasnich R 1993 Bone mass measurement: Prediction of risk. Am J Med 95:6S–10S.

45. Fijneman RJ, de Vries SS, Jansen RC, Demant P 1996 Complex interactions of new quantitative trait loci, Sluc1, Sluc2, Sluc3, and Sluc4, that influence the susceptibility to lung cancer in the mouse. Nat Genet 14:465–467.

46. van Wezel T, Stassen AP, Moen CJ, Hart AA, van der Valk MA, Demant P 1996 Gene interaction and single gene effects in colon tumour susceptibility in mice. Nat Genet 14:468–470.

47. Beamer WG, Shultz KL, Churchill GA, Frankel WN, Baylink DJ, Rosen CJ, Donahue LR 1999 Quantitative trait loci for bone density in C57BL/6J and CAST/EiJ inbred mice. Mamm Genome 10:1043–1049.

48. Beamer WG, Rosen CJ, Donahue LR, Frankel WN, Churchill GA, Shultz KL, Baylink DJ, Pettis JL 1998 Location of genes regulating volumetric bone mineral density in C57BL/6J (low) and C3H/HeJ (high) inbred strains of mice. ASBMR-IBMS Second Joint Meeting, Bone, vol. 23, San Francisco, CA, USA, p. S162.

49. Shimizu M, Higuchi K, Bennett B, Xia C, Tsuboyama T, Kasai S, Chiba T, Fujisawa H, Kogishi K, Kitado H, Kimoto M, Takeda N, Matsushita M, Okumura H, Serikawa T, Nakamura T, Johnson TE, Hosokawa M 1999 Identification of peak bone mass QTL in a spontaneously osteoporotic mouse strain. Mamm Genome 10:81–87.

50. Benes H, Weinstein RS, Zheng W, Thaden JJ, Jilka RL, Manolagas SC, Shmookler Reis RJ 2000 Chromosomal mapping of osteopenia-associated quantitative trait loci using closely related mouse strains. J Bone Miner Res 15:626–633.

51. Klein RF, Mitchell SR, Phillips TJ, Belknap JK, Orwoll ES 1998 Quantitative trait loci affecting peak bone mineral density in mice. J Bone Miner Res 13:1648–1656.

52. Johnson ML, Gong G, Kimberling W, Recker SM, Kimmel DB, Recker RB 1997 Linkage of a gene causing high bone mass to human chromosome 11 (11q12–13). Am J Hum Genet 60:1326–1332.

53. Koller DL, Rodriguez LA, Christian JC, Slemenda CW, Econs MJ, Hui SL, Morin P, Conneally PM, Joslyn G, Curran ME, Peacock M, Johnston CC, Foroud T 1998 Linkage of a QTL contributing to normal variation in bone mineral density to chromosome 11q12–13. J Bone Miner Res 13:1903–1908.

54. Wasnich RD, Davis JW, Ross PD 1994 Spine fracture risk is predicted by non-spine fractures. Osteoporos Int 4:1–5.

55. Myers ER, Hecker AT, Rooks DS, Hipp JA, Hayes WC 1993 Geometric variables from DXA of the radius predict forearm fracture load in vitro. Calcif Tissue Int 52:199–204.

56. Boonen S, Koutri R, Dequeker J, Aerssens J, Lowet G, Nijs J, Verbeke G, Lesaffre E, Geusens P 1995 Measurement of femoral geometry in type I and type II osteoporosis: Differences in hip axis length consistent with heterogeneity in the

AQ: 8

AQ: 9

AQ: 10

AQ: 11

AQ: 12

pathogenesis of osteoporotic fractures. J Bone Miner Res **10:**1908–1912.

57. Faulkner KG, Cummings SR, Black D, Palermo L, Gluer CC, Genant HK 1993 Simple measurement of femoral geometry predicts hip fracture: The study of osteoporotic fractures. J Bone Miner Res **8:**1211–1217.

58. Faulkner KG, McClung M, Cummings SR 1994 Automated evaluation of hip axis length for predicting hip fracture. J Bone Miner Res **9:**1065–1070.

59. Flicker L, Faulkner KG, Hopper JL, Green RM, Kaymacki B, Nowson CA, Young D, Wark JD 1996 Determinants of hip axis length in women aged 10–89 years: A twin study. Bone **18:**41–45.

60. Gluer CC, Cummings SR, Pressman A, Li J, Gluer K, Faulkner KG, Grampp S, Genant HK 1994 Prediction of hip fractures from pelvic radiographs: The study of osteoporotic fractures. The Study of Osteoporotic Fractures Research Group. J Bone Miner Res **9:**671–677.

61. Mikhail MB, Vaswani AN, Aloia JF 1996 Racial differences in femoral dimensions and their relation to hip fracture. Osteoporos Int **6:**22–24.

62. Nakamura T, Turner CH, Yoshikawa T, Slemenda CW, Peacock M, Burr DB, Mizuno Y, Orimo H, Ouchi Y, Johnston CJ 1994 Do variations in hip geometry explain differences in hip fracture risk between Japanese and white Americans? J Bone Miner Res **9:**1071–1076.

63. O'Neill TW, Grazio S, Spector TD, Silman AJ 1996 Geometric measurements of the proximal femur in UK women: Secular increase between the late 1950s and early 1990s. Osteoporos Int **6:**136–140.

64. Reid IR, Chin K, Evans MC, Jones JG 1994 Relation between increase in length of hip axis in older women between 1950s and 1990s and increase in age specific rates of hip fracture. BMJ **309:**508–509.

65. Reid IR, Chin K, Evans MC, Cundy T 1996 Longer femoral necks in the young: A predictor of further increases in hip fracture incidence? N Z Med J **109:**234–235.

66. van der Meulen MC, Ashford MW Jr, Kiratli BJ, Bachrach LK, Carter DR 1996 Determinants of femoral geometry and structure during adolescent growth. J Orthop Res **14:**22–29.

67. Bell KL, Loveridge N, Power J, Garrahan N, Stanton M, Lunt M, Meggitt BF, Reeve J 1999 Structure of the femoral neck in hip fracture: Cortical bone loss in the inferoanterior to superoposterior axis. J Bone Miner Res **14:**111–1119.

68. Bell KL, Loveridge N, Power J, Garrahan N, Meggitt BF, Reeve J 1999 Regional differences in cortical porosity in the fractured femoral neck. Bone **24:**57–64.

69. Duan Y, Parfitt A, Seeman E 1999 Vertebral bone mass, size, and volumetric density in women with spinal fractures. J Bone Miner Res **14:**1796–1802.

70. Akhter MP, Cullen DM, Pedersen EA, Kimmel DB, Recker RR 1998 Bone response to in vivo mechanical loading in two breeds of mice. Calcif Tissue Int **63:**442–449.

71. Bhudhikanok GS, Wang MC, Eckert K, Matkin C, Marcus R, Bachrach LK 1996 Differences in bone mineral in young Asian and Caucasian Americans may reflect differences in bone size. J Bone Miner Res **11:**1545–1556.

72. Cummings SR, Cauley JA, Palermo L, Ross PD, Wasnich RD, Black D, Faulkner KG 1994 Racial differences in hip axis lengths might explain racial differences in rates of hip fracture.

73. Seeman E 1998 Growth in bone mass and size—are racial and gender differences in bone mineral density more apparent than real? J Clin Endocrinol Metab **83:**1414–1419.

74. Seeman E 1999 The structural basis of bone fragility in men. Bone **25:**143–147.

75. Niu T, Chen C, Cordell H, Yang J, Wang B, Wang Z, Fang Z, Schork NJ, Rosen CJ, Xu X 1999 A genome-wide scan for loci linked to forearm bone mineral density. Hum Genet **104:**226–233.

76. Katzman DK, Bachrach LK, Carter DR, Marcus R 1991 Clinical and anthropometric correlates of bone mineral acquisition in healthy adolescent girls. J Clin Endocrinol Metab **73:**1332–1339.

77. Bonjour JP, Theintz G, Law F, Slosman D, Rizzoli R 1994 Peak bone mass. Osteoporos Int 4(Suppl 1):7–13.

78. Bass S, Delmas PD, Pearce G, Hendrich E, Tabensky A, Seeman E 1999 The differing tempo of growth in bone size, mass, and density in girls is region-specific. J Clin Invest **104:**795–804.

79. Zamberlan N, Radetti G, Paganini C, Gatti D, Rossini M, Braga V, Adami S 1996 Evaluation of cortical thickness and bone density by roentgen microdensitometry in growing males and females. Eur J Pediatr **155:**377–382.

80. Gilsanz V, Boechat MI, Gilsanz R, Loro ML, Roe TF, Goodman WG 1994 Gender differences in vertebral sizes in adults: Biomechanical implications. Radiology **190:**678–682.

81. Gilsanz V, Loro ML, Roe TF, Sayre J, Gilsanz R, Schulz EE 1995 Vertebral size in elderly women with osteoporosis. Mechanical implications and relationship to fractures. J Clin Invest **95:**2332–2337.

82. Nadeau JH 1989 Maps of linkage and synteny homologies between mouse and man. Trends Genet **5:**82–86.

83. Eppig JT, Nadeau JH 1995 Comparative maps: The mammalian jigsaw puzzle. Curr Opin Genet Dev **5:**709–716.

84. DeBry RW, Seldin MF 1996 Human/mouse homology relationships. Genomics **33:**337–351.

85. Seldin MF 1997 Human/Mouse Homology Relationships. National Center for Biotechnology Information, Bethesda, MD, and Davis, CA, USA.

86. Takeda T, Hosokawa M, Higuchi K 1991 Senescence-accelerated mouse (SAM): A novel murine model of accelerated senescence. J Am Geriatr Soc **39:**911–919.

87. Frost HM, Jee WSS 1992 On the rat model of human osteopenias and osteoporoses. Bone Miner **18:**227–236.

88. Blank RD, Campbell GR, D'Eustachio P 1986 Possible derivation of the laboratory mouse genome from multiple wild Mus species. Genetics **114:**1257–1269.

AQ: 13

University of Wisconsin Medical School H4/556 CSC (5148) 600 Highland Ave. Madison, WI 53792 (should this be listed on p1 as my present address?)

Moved during review of this paper.

Department of
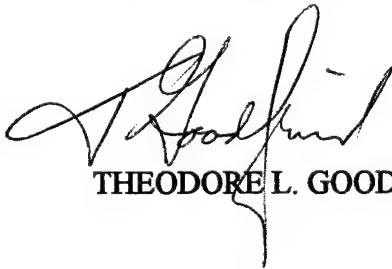Veterans Affairs

Memorandum

Date: November 16, 2000

From: Associate Chief of Staff for Research

Subj: Research Protocol

To: Robert Blank, M.D.

1. Your animal protocol "Genetics of Bone Strength in HcB/Dem Mice:
Intercrosses of Highly Divergent HcB Strains" was reviewed and approved by the
VA Research and Development Committee on November 7, 2000.

2. The protocol was approved by the VA Animal Research Committee on
October 18, 2000.

3. The R&D Committee also approved the acceptance of any funding that may
accompany this study. If you intend to have funds for this study deposited in a
VA account, contact Marvin Rupp (ext. 17801) to make arrangements.

THEODORE L. GOODFRIEND, M.D.

MEMORANDUM

TO: Dr. Robert Blank

FROM: Rick Lane
            Associate Director

DATE: April 10, 2001

RE: Animal Protocol – M01525

Dr. Blank,

This memo is to provide documentation as to approvals for your animal based research: **Genetics of Bone Strength in HcB/Dem Mice: Intercrosses of Highly Divergent HcB Strains**. The protocol covering this project was originally approved by the Middleton V.A. Hospital Animal Care Committee on October 18, 2000. In January 2001, with the V.A. animal facility unable to provide the necessary type of housing, the University Hospital animal care unit was contacted as a possible alternate site. As there was available space, the chair and attending veterinarian from the Medical School Animal Care and Use Committee reviewed the V.A. approved protocol and approved the animal housing. Those animals were moved into the University facility on 1/26/01.

With many researchers having joint appointments, the Middleton V.A. and University of Wisconsin Medical School Animal Care Committees have a long standing cooperative arrangement for dealing with and assuring appropriate approval of protocols. This cooperation includes such things as the acceptance of each other's protocol formats; the shared investment/management of specialized facilities; and cooperative training programs. To provide a cross reference, V.A. protocols are assigned a U.W. protocol number. For your protocol, that number is: A-53-4245-M01525-3-03-01. If there are any questions, please feel free to contact me, 262-0400.

Cc: Dr. James Southard

Research Animal Resources Center

396 Enzyme Institute   University of Wisconsin–Madison   1710 University Avenue   Madison, Wisconsin 53705–4098
608/262–1238   FAX: 608/265–2698

Breaking Down Bone Strength
A Perspective on the Future of Skeletal Genetics

Robert D. Blank
University of Wisconsin Medical School
Endocrinology Section, Department of Medicine
H4/556 CSC (5148)
600 Highland Ave.
Madison, WI 53792
Phone: (608) 262-5586
Fax: (608) 265-0462
e-mail: rdb@medicine.wisc.edu

Understanding the basis of skeletal fragility is one of the major goals pursued by readers of the *Journal of Bone and Mineral Research*. Over the past decade, genetic approaches have become increasingly prominent in addressing this problem. This month's issue of the journal includes a report by Beamer and associates [1] identifying quantitative trait loci (QTLs) for femoral and vertebral volumetric bone mineral density (vBMD). Placing their work in context presents an opportunity to reflect on recent progress in bone genetics and on the field's future directions.

Choice of Phenotypes

Fracture, not BMD, is the clinically relevant outcome and BMD is only one of several parameters related to biomechanical performance. Therefore, in the ideal situation, one would wish to perform genetic analyses directly on fracture rather than on surrogate traits that correlate imperfectly with fracture. Deng and colleagues [2] estimated that the narrow-sense heritability of Colle's fracture was about 0.25 in a cohort of white American women, meaning that genetic constitution accounted for approximately ¼ of total Colle's fracture risk variation observed. While this result indicates that the magnitude of the genetic contribution to fracture is sufficiently large to be fruitfully pursued, important caveats must be noted. Fractures are relatively rare and tend to occur late in life. Should the genetic basis of human fracture prove to be quantitative, then the contributions of individual loci to the total fracture risk are likely to be too small to allow individual QTLs to be mapped successfully with realistic sample sizes. These considerations impose important, and possibly insurmountable, obstacles to recruiting an adequate population to perform mapping studies of Colle's fracture in humans. Colle's fractures are frequent relative to hip fractures, so the challenge of collecting an adequate sample to perform equivalent analyses of hip fracture would be an even more daunting challenge.

Vertebral fractures, while relatively common, do not always come to clinical attention (e.g. [3,4]) and are subject to a degree of diagnostic uncertainty [5-9], posing potential problems in their study.

Investigators have adopted alternative strategies based on the use surrogate endpoints to overcome the practical limitations of studying human fracture directly. One approach is to study biomechanical performance in a contrived experimental scheme as an analogue for natural fracture. This approach has the virtue of allowing functional assessment of the bone, but is limited insofar as the fracture mechanisms in biomechanical testing differ from those of naturally occurring fractures. Moreover, these investigations are generally performed using cadaver specimens or specimens obtained from model organisms, imposing additional differences from *in vivo* human fractures. A second approach is based on epidemiologic data and focuses on predictors of fracture rather than analogues of fracture. The vast literature on densitometric assessment of bone by various modalities is representative of this strategy. The same logic underlies investigations based on instruments assessing lifestyle factors, comorbidities, and mobility. The success of these methods is incontrovertible; indeed the WHO diagnostic criteria for osteoporosis rely primarily on densitometric assessment [10]. In addition, there is broad agreement in the community regarding the risk factors for fracture (e.g. [11,12]). A closer look at the risk factor based literature reveals important limitations as well. As in the case of vertebral fracture, markers of fracture risk are variously defined, and while they are related, they are nevertheless distinct. This is readily apparent when comparing densitometric parameters– cross-calibrating fracture risk based on T scores obtained by different techniques at different sites [13-19] poses an important problem in patient care. Similarly, there is considerable overlap among the

data included in assessments of clinical risk factors for fracture, but cross-calibration across instruments has not yet been achieved.

At least as important a limitation of this approach is that optimizing predictive ability does not necessarily advance mechanistic understanding of fracture biology, a point that warrants further elaboration. Areal BMD (aBMD) measured by dual energy X ray absorptiometry (DEXA) is the single best predictor of fracture risk at the studied site (using lateral view at the spine). It is well established that large bones have higher aBMDs than small bones having equal vBMD (e.g. [20]) due to projection artifact. It is also well established that larger bones are stronger than smaller bones having equivalent tissue strength. By combining both size and mineral density into a single measure, aBMD achieves better fracture prediction than does vBMD, in which the contribution of bone size is explicitly removed from consideration. Yet, understanding the underlying bone biology requires that bone size and BMD be treated as distinct properties [21-23].

In contrast, the biomechanical approach (reviewed by [24,25]) seeks to partition performance into components that promote investigation of mechanisms. The most basic distinction is that between structural and material properties. Structural properties are those possessed by an entire bone, and are determined jointly by its anatomy and its tissue strength. The material properties are those of the bone tissue *per se*, after correction for differences in anatomy. Distinct components of biomechanical performance can also be identified in interpreting the load-deformation curve obtained in testing a specimen. It is also important to note that each of these properties has a corresponding material parameter obtained by normalizing for anatomy. Additional mechanical properties can also be obtained by different testing schemes; for example, repetitive, low intensity loading can be used to assess fatigue.

Similarly, the anatomic component of structural strength can be divided further. The distinction between cortical and trabecular bone is familiar to readers of the *Journal*, as are ongoing efforts to quantify various architectural bone properties.

While the framework provided by biomechanics naturally leads to efforts to analyze bone strength into ever more refined components, such partition is not always easily achieved in practice. Because bone is an anisotropic tissue, its biomechanical performance will vary according to the orientation of the tissue relative to the applied load (e.g. [26,27]). This overlap between anatomic and tissue components is particularly evident in considering trabecular bone e.g. [28-30]). Even given these limitations, a reductionistic program explicitly pursues mechanistic understanding.

Adopting the reductionistic approach embodied by biomechanics does not require that we abandon epidemiology. Both epidemiologic and interventional investigations have identified risk factors for fracture other than bone mass. Advancing age [31,32]), past personal atraumatic fracture history (eg [11,33-35]), and maternal hip fracture history [12] each increase fracture risk. In trials of alendronate and transdermal estrogen, the fracture benefit exceeded that predicted from the observed BMD increase [36,37]. In contrast, treatment with sodium fluoride has been shown to increase BMD, but either not to improve or to worsen fracture outcomes [38,39]. Taken together, these data demonstrate that factors other than BMD, often referred to collectively as bone quality, contribute to the material strength of bone, thereby linking these disparate research areas.

Linkage Genetics of Bone: Present Status

Several different strategies have been used to study skeletal genetics. While each provides a potentially valuable approach, the different types of studies address somewhat different questions [40]. Only linkage studies are considered here, addressing the question "where

are genes (loci) whose segregation contributes to differences in the trait of interest located?" In human samples, this question is distinct from that of identifying which allele of that gene is responsible for different values of the trait. In contrast, the existence of inbred mouse lines allow investigation of both loci and alleles to be accomplished simultaneously [41].

In humans, a locus conferring high BMD as a simple Mendelian trait has successfully been mapped [42]. Investigations by another research group implicate the same genomic region as a QTL contributing to less dramatic variation in BMD [43,44]. Two other human genome scans reported evidence of possible linkage for hip and spine [45] and forearm [46]. It is worth noting that both of these investigations found evidence for a QTL on chromosome 2p in spite of the different sites and populations studied. Each of these studies used aBMD as the phenotypic endpoint, based on the ease, economy, safety, and acceptance of aBMD as a surrogate measure of skeletal fragility.

In mice, a broader range of phenotypes has been studied. Klein et al. [47] studied whole body aBMD in the B X D recombinant inbred lines. Benes and colleagues [48] used DEXA scanning studying vertebral aBMD in a pair of crosses between SAMP6 and either SAMR2 or AKR/J. Shimizu and co-workers [49] studied femoral cortical thickness index, the fraction of diaphyseal cross-section occupied by cortical bone on plain radiographs, in a cross between SAMP6 and SAMP2. Beamer and colleagues have reported two related studies, a cross between C57BL/6J and Cast/EiJ in which femoral vBMD was mapped [50] and a study of IGF-1 levels in a cross between C57BL/6J and C3H/HeJ [51]. Yershov et al. [52] examined humeral biomechanical performance and dimensions, ash percentage, and body mass in the HcB/Dem recombinant congenic strains.

In this issue, Beamer *et al.* present the results of mapping femoral and vertebral vBMD in a cross between C57BL/6J and C3H/HeJ [1]. Their results are notable for several reasons. First, a subset of the QTLs contributes to vBMD at both sites studied, while others contribute to vBMD at only one site. This finding provides a biological context for the clinical finding of disparate BMDs at different sites in the same individual. Second, in several cases the same QTLs have been mapped in different crosses, using different but related phenotypes. This provides compelling evidence that a bone mass gene is in fact being identified. Third, the number of individuals studied in this cross was sufficient to allow testing for pairwise epistatic interactions, which were not found. Although it is too soon to say that epistasis does not contribute signficantly to vBMD variation in general, this group's efforts remind the rest of us that gene-gene and gene-environment interactions should be sought. Fourth, the authors are unequivocal in stating their ambition to use linkage studies to help elucidate the mechanisms underlying bone phenotypes, placing them in the reductionist camp.

The future of Skeletal Genetics

Successfully mapping QTLs is a relatively early step in understanding the genetic basis of skeletal function. Now that the approximate locations of some vBMD QTLs are known, we are faced with the problem of identifying which of the positional candidates thus defined are the relevant genes. Similar research efforts in other diseases, notably type I diabetes (e.g. [53-55]) and other autoimmune diseases (e.g. [56-58]), suggest that successfully subdividing the overall phenotype into pathophysiologically relevant intermediate phenotypes is one of the major tasks that lies ahead. Jepsen *et al.* [59] report an elegant example of this approach in a forthcoming issue (please specify issue, if known) of the *Journal*. Subdivision of traits may lead to phenotypes whose genetics are Mendelian rather than quantitative, greatly simplifying their

genetic analysis, as illustrated by the high bone mass locus [42]. Even if reduction to oligogenic phenotypes is not accomplished, the discussion generated in our community through the effort will undoubtedly stimulate new ideas about how whole-bone anatomy is established, how bone responds to mechanical loading, how matrix proteins and minerals interact, and how bone metabolism changes during development and aging. Each of these is already an active research area; and their findings need to be more integrated into genetic investigations of fracture risk and its components, including BMD. Choosing among the myriad potential intermediate phenotypes to study will depend largely on this ongoing discussion. A second thread contributing to choice among intermediate phenotypes will be based on technical issues. New instruments and new analytical methods provide opportunities to define additional phenotypes (e.g. [60-63]).

Work to date has already employed a variety of different albeit related phenotypes. Study of intermediate phenotypes, as proposed above, will add still more traits into the mix. This presents us with the additional challenge of relating the phenotypes to each other. A potential approach to this problem is to design future genetic experiments to include a variety of traits and then seek evidence of pleiotropy, *i.e.* a single gene controlling multiple phenotypes [52,64,65]. The data presented by Beamer and colleagues [1] contribute to this effort by distinguishing between QTLs acting at both femur and spine and QTLs acting in a site-specific manner. Orwoll and colleagues' studies [66] of gender specific BMD QTLs apply this approach also.

Finally, progress in genomics favors investigations based on interesting and insightful biology. Recent completion of the human genome sequence [67] and the pending completion of the mouse and rat sequences will devalue some of the skills geneticists have mastered. High density maps and microarray technologies will allow adoption of multi-generational association

analyses having greater statistical power than traditional linkage methods [68]. These advances demand that the bone geneticists of the future be bone biologists first. This issue's paper by Beamer et al. [1] points the way ahead.

Acknowledgment

References

1.	Beamer WG, Shultz KL, Donahue LR, Churchill GA, Sen S, Wergedal JR, Baylink DJ, Rosen CJ 2001 Quantitative trait loci for femoral and lumbar vertebral bone mineral density in C57BL/6J and C3H/HeJ inbred strains of mice. J Bone Miner Res **16**:???

2.	Deng HW, Chen WM, Recker S, Stegman MR, Li JL, Davies KM, Zhou Y, Deng H, Heaney R, Recker RR 2000 Genetic determination of Colles' fracture and differential bone mass in women with and without Colles' fracture. J Bone Miner Res **15**(7):1243-52.

3.	Ettinger B, Black DM, Nevitt MC, Rundle AC, Cauley JA, Cummings SR, Genant HK 1992 Contribution of vertebral deformities to chronic back pain and disability. The Study of Osteoporotic Fractures Research Group. J Bone Miner Res **7**(4):449-56.

4.	Nevitt MC, Ettinger B, Black DM, Stone K, Jamal SA, Ensrud K, Segal M, Genant HK, Cummings SR 1998 The association of radiographically detected vertebral fractures with back pain and function: a prospective study. Ann Intern Med **128**(10):793-800.

5. Minne HW, Leidig G, Wuster C, Siromachkostov L, Baldauf G, Bickel R, Sauer P, Lojen M, Ziegler R 1988 A newly developed spine deformity index (SDI) to quantitate vertebral crush fractures in patients with osteoporosis. Bone Miner 3(4):335-49.

6. Melton LJd, Kan SH, Frye MA, Wahner HW, WM OF, Riggs BL 1989 Epidemiology of vertebral fractures in women. Am J Epidemiol 129(5):1000-11.

7. Eastell R, Cedel SL, Wahner HW, Riggs BL, Melton LJd 1991 Classification of vertebral fractures. J Bone Miner Res 6(3):207-15.

8. Ross PD, Yhee YK, He YF, Davis JW, Kamimoto C, Epstein RS, Wasnich RD 1993 A new method for vertebral fracture diagnosis. J Bone Miner Res 8(2):167-74.

9. McCloskey EV, Spector TD, Eyres KS, Fern ED, N OR, Vasikaran S, Kanis JA 1993 The assessment of vertebral deformity: a method for use in population studies and clinical trials. Osteoporos Int 3(3):138-47.

10. 1994 Assessment of fracture risk and its application to screening for postmenopausal osteoporosis. Report of a WHO Study Group. World Health Organ Tech Rep Ser 843:1-129.

11. Ross PD, Davis JW, Wasnich RD 1993 Bone mass and beyond: risk factors for fractures. Calcif Tissue Int 53 Suppl 1:S134-7; discussion S137-8.

12. Cummings SR, Nevitt MC, Browner WS, Stone K, Fox KM, Ensrud KE, Cauley J, Black D, Vogt TM 1995 Risk factors for hip fracture in white women. Study of Osteoporotic Fractures Research Group. N Engl J Med 332(12):767-73.

13. Martin JC, Reid DM 1996 Appendicular measurements in screening women for low axial bone mineral density. Br J Radiol 69(819):234-40.

14.   Takada M, Engelke K, Hagiwara S, Grampp S, Jergas M, Gluer CC, Genant HK 1997 Assessment of osteoporosis: comparison of radiographic absorptiometry of the phalanges and dual X-ray absorptiometry of the radius and lumbar spine. Radiology **202**(3):759-63.

15.   Grampp S, Genant HK, Mathur A, Lang P, Jergas M, Takada M, Gluer CC, Lu Y, Chavez M 1997 Comparisons of noninvasive bone mineral measurements in assessing age-related loss, fracture discrimination, and diagnostic classification. J Bone Miner Res **12**(5):697-711.

16.   Yeap SS, Pearson D, Cawte SA, Hosking DJ 1998 The relationship between bone mineral density and ultrasound in postmenopausal and osteoporotic women. Osteoporos Int **8**(2):141-6.

17.   Frost ML, Blake GM, Fogelman I 1999 Contact quantitative ultrasound: an evaluation of precision, fracture discrimination, age-related bone loss and applicability of the WHO criteria. Osteoporos Int **10**(6):441-9.

18.   Guglielmi G, Cammisa M, De Serio A, Scillitani A, Chiodini I, Carnevale V, Fusilli S 1999 Phalangeal US velocity discriminates between normal and vertebrally fractured subjects. Eur Radiol **9**(8):1632-7.

19.   Faulkner KG, von Stetten E, Miller P 1999 Discordance in patient classification using T-scores. J Clin Densitom **2**(3):343-50.

20.   Jergas M, Breitenseher M, Gluer CC, Yu W, Genant HK 1995 Estimates of volumetric bone density from projectional measurements improve the discriminatory capability of dual X-ray absorptiometry. J Bone Miner Res **10**(7):1101-10.

21. Bass S, Delmas PD, Pearce G, Hendrich E, Tabensky A, Seeman E 1999 The differing tempo of growth in bone size, mass, and density in girls is region-specific. J Clin Invest **104**(6):795-804.

22. Duan Y, Parfitt A, Seeman E 1999 Vertebral bone mass, size, and volumetric density in women with spinal fractures. J Bone Miner Res **14**(10):1796-802.

23. Gilsanz V, Loro ML, Roe TF, Sayre J, Gilsanz R, Schulz EE 1995 Vertebral size in elderly women with osteoporosis. Mechanical implications and relationship to fractures. J Clin Invest **95**(5):2332-7.

24. Hayes W 1986 Basic Biomechanics of the Skeleton Current Concepts of Bone Fragility. Springer-Verlag, Heidelberg, pp 3-18.

25. Turner CH, Burr DB 1993 Basic biomechanical measurements of bone: a tutorial. Bone **14**(4):595-608.

26. Martin RB, Ishida J 1989 The relative effects of collagen fiber orientation, porosity, density, and mineralization on bone strength. J Biomech **22**(5):419-26.

27. Martin RB, Boardman DL 1993 The effects of collagen fiber orientation, porosity, density, and mineralization on bovine cortical bone bending properties. J Biomech **26**(9):1047-54.

28. Goulet RW, Goldstein SA, Ciarelli MJ, Kuhn JL, Brown MB, Feldkamp LA 1994 The relationship between the structural and orthogonal compressive properties of trabecular bone. J Biomech **27**(4):375-89.

29. Muller R, Hahn M, Vogel M, Delling G, Ruegsegger P 1996 Morphometric analysis of noninvasively assessed bone biopsies: comparison of high-resolution computed tomography and histologic sections. Bone **18**(3):215-20.

30. Augat P, Link T, Lang TF, Lin JC, Majumdar S, Genant HK 1998 Anisotropy of the elastic modulus of trabecular bone specimens from different anatomical locations. Med Eng Phys **20**(2):124-31.

31. Paganini-Hill A, Chao A, Ross RK, Henderson BE 1991 Exercise and other factors in the prevention of hip fracture: the Leisure World study. Epidemiology **2**(1):16-25.

32. Graafmans WC, Ooms ME, Bezemer PD, Bouter LM, Lips P 1996 Different risk profiles for hip fractures and distal forearm fractures: a prospective study. Osteoporos Int **6**(6):427-31.

33. Ross PD, Davis JW, Epstein RS, Wasnich RD 1991 Pre-existing fractures and bone mass predict vertebral fracture incidence in women. Ann Intern Med **114**(11):919-23.

34. Kotowicz MA, Melton LJ, 3rd, Cooper C, Atkinson EJ, WM OF, Riggs BL 1994 Risk of hip fracture in women with vertebral fracture. J Bone Miner Res **9**(5):599-605.

35. Wasnich RD, Davis JW, Ross PD 1994 Spine fracture risk is predicted by non-spine fractures. Osteoporos Int **4**(1):1-5.

36. Lufkin EG, Wahner HW, WM OF, Hodgson SF, Kotowicz MA, Lane AW, Judd HL, Caplan RH, Riggs BL 1992 Treatment of postmenopausal osteoporosis with transdermal estrogen. Ann Intern Med **117**(1):1-9.

37. Liberman UA, Weiss SR, Broll J, Minne HW, Quan H, Bell NH, Rodriguez-Portales J, Downs RW, Jr., Dequeker J, Favus M 1995 Effect of oral alendronate on bone mineral density and the incidence of fractures in postmenopausal osteoporosis. The Alendronate Phase III Osteoporosis Treatment Study Group. N Engl J Med **333**(22):1437-43.

38. Hedlund LR, Gallagher JC 1989 Increased incidence of hip fracture in osteoporotic women treated with sodium fluoride. J Bone Miner Res **4**(2):223-5.

39.   Riggs BL, Hodgson SF, WM OF, Chao EY, Wahner HW, Muhs JM, Cedel SL, Melton LJd 1990 Effect of fluoride treatment on the fracture rate in postmenopausal women with osteoporosis. N Engl J Med **322**(12):802-9.

40.   Blank RD 1999 Linkage, Association, and the Genetic Analysis of Bone Mineral Density and Related Phenotypes: an Overview for Clinicians. J Clin Densitom **2**(1):59-70.

41.   Lander E, Schork N 1994 Genetic Dissection of Complex Traits. Science **265**:2038-2048.

42.   Johnson ML, Gong G, Kimberling W, Recker SM, Kimmel DB, Recker RB 1997 Linkage of a gene causing high bone mass to human chromosome 11 (11q12-13). Am J Hum Genet **60**(6):1326-32.

43.   Koller DL, Rodriguez LA, Christian JC, Slemenda CW, Econs MJ, Hui SL, Morin P, Conneally PM, Joslyn G, Curran ME, Peacock M, Johnston CC, Foroud T 1998 Linkage of a QTL contributing to normal variation in bone mineral density to chromosome 11q12-13. J Bone Miner Res **13**(12):1903-8.

44.   Koller DL, Econs MJ, Morin PA, Christian JC, Hui SL, Parry P, Curran ME, Rodriguez LA, Conneally PM, Joslyn G, Peacock M, Johnston CC, Foroud T 2000 Genome screen for QTLs contributing to normal variation in bone mineral density and osteoporosis. J Clin Endocrinol Metab **85**(9):3116-20.

45.   Devoto M, Shimoya K, Caminis J, Ott J, Tenenhouse A, Whyte MP, Sereda L, Hall S, Considine E, Williams CJ, Tromp G, Kuivaniemi H, Ala-Kokko L, Prockop DJ, Spotila LD 1998 First-stage autosomal genome screen in extended pedigrees suggests genes predisposing to low bone mineral density on chromosomes 1p, 2p and 4q. Eur J Hum Genet **6**(2):151-7.

46. Niu T, Chen C, Cordell H, Yang J, Wang B, Wang Z, Fang Z, Schork NJ, Rosen CJ, Xu X 1999 A genome-wide scan for loci linked to forearm bone mineral density. Hum Genet **104**(3):226-33.

47. Klein RF, Mitchell SR, Phillips TJ, Belknap JK, Orwoll ES 1998 Quantitative trait loci affecting peak bone mineral density in mice. J Bone Miner Res **13**(11):1648-56.

48. Benes H, Weinstein RS, Zheng W, Thaden JJ, Jilka RL, Manolagas SC, Shmookler Reis RJ 2000 Chromosomal mapping of osteopenia-associated quantitative trait loci using closely related mouse strains. J Bone Miner Res **15**(4):626-33.

49. Shimizu M, Higuchi K, Bennett B, Xia C, Tsuboyama T, Kasai S, Chiba T, Fujisawa H, Kogishi K, Kitado H, Kimoto M, Takeda N, Matsushita M, Okumura H, Serikawa T, Nakamura T, Johnson TE, Hosokawa M 1999 Identification of peak bone mass QTL in a spontaneously osteoporotic mouse strain. Mamm Genome **10**(2):81-7.

50. Beamer WG, Shultz KL, Churchill GA, Frankel WN, Baylink DJ, Rosen CJ, Donahue LR 1999 Quantitative trait loci for bone density in C57BL/6J and CAST/EiJ inbred mice. Mamm Genome **10**(11):1043-9.

51. Rosen CJ, Churchill GA, Donahue LR, Shultz KL, Burgess JK, Powell DR, Beamer WG 2000 Mapping quantitative trait loci for serum insulin-like growth factor-1 levels in mice. Bone **27**(4):521-8.

52. Yershov Y, Baldini TH, Villagomez S, Young T, Martin ML, Bockman RS, Peterson MGE, Blank RD 2001 Bone Strength and Related Traits in HcB/Dem Recombinant Congenic Mice. J Bone Miner Res **16**:???

53. Todd JA 1999 From genome to aetiology in a multifactorial disease, type 1 diabetes. Bioessays **21**(2):164-74.

54. Paterson AD, Petronis A 2000 Age of diagnosis-based linkage analysis in type 1 diabetes. Eur J Hum Genet **8**(2):145-8.

55. Becker KG 1999 Comparative genetics of type 1 diabetes and autoimmune disease: common loci, common pathways? Diabetes **48**(7):1353-8.

56. Postma DS, Bleecker ER, Amelung PJ, Holroyd KJ, Xu J, Panhuysen CI, Meyers DA, Levitt RC 1995 Genetic susceptibility to asthma--bronchial hyperresponsiveness coinherited with a major gene for atopy. N Engl J Med **333**(14):894-900.

57. Daniels SE, Bhattacharrya S, James A, Leaves NI, Young A, Hill MR, Faux JA, Ryan GF, le Souef PN, Lathrop GM, Musk AW, Cookson WO 1996 A genome-wide search for quantitative trait loci underlying asthma. Nature **383**(6597):247-50.

58. Morel L, Wakeland EK 2000 Lessons from the NZM2410 model and related strains. Int Rev Immunol **19**(4-5):423-46.

59. Jepsen KJ, Pennington DE, Lee YL, Warman M, Nadeau J 2001 Bone Brittleness Varies with Genetic Background in A/J and C57BL/6J Inbred Mice. J Bone Miner Res **16**:accepted? E0011 565.

60. Marcott C, Reeder RC, Paschalis EP, Tatakis DN, Boskey AL, Mendelsohn R 1998 Infrared microspectroscopic imaging of biomineralized tissues using a mercury-cadmium-telluride focal-plane array detector. Cell Mol Biol (Noisy-le-grand) **44**(1):109-15.

61. Majumdar S, Link TM, Millard J, Lin JC, Augat P, Newitt D, Lane N, Genant HK 2000 In vivo assessment of trabecular bone structure using fractal analysis of distal radius radiographs. Med Phys **27**(11):2594-9.

62. Laib A, Hildebrand T, Hauselmann HJ, Ruegsegger P 1997 Ridge number density: a new parameter for in vivo bone structure analysis. Bone **21**(6):541-6.

63. Smit TH, Schneider E, Odgaard A 1998 Star length distribution: a volume-based concept for the characterization of structural anisotropy. J Microsc **191**(Pt 3)(6):249-57.

64. Comuzzie AG, Mahaney MC, Almasy L, Dyer TD, Blangero J 1997 Exploiting pleiotropy to map genes for oligogenic phenotypes using extended pedigree data. Genet Epidemiol **14**(6):975-80.

65. Rogers J, Mahaney MC, Beamer WG, Donahue LR, Rosen CJ 1997 Beyond one gene-one disease: alternative strategies for deciphering genetic determinants of osteoporosis. Calcif Tissue Int **60**(3):225-8.

66. Orwoll ES, Belknap JK, Klein RF 2001 Gender Specificity in the Genetic Determinants of Peak Bone Mass. J Bone Miner Res **16**:submitted 0010 537 (accepted?).

67. Venter JC, Adams MD, Myers EW, Li PW, Mural RJ, Sutton GG, Smith HO, Yandell M, Evans CA, Holt RA, Gocayne JD, Amanatides P, Ballew RM, Huson DH, Wortman JR, Zhang Q, Kodira CD, Zheng XH, Chen L, Skupski M, Subramanian G, Thomas PD, Zhang J, Gabor Miklos GL, Nelson C, Broder S, Clark AG, Nadeau J, McKusick VA, Zinder N, Levine AJ, Roberts RJ, Simon M, Slayman C, Hunkapiller M, Bolanos R, Delcher A, Dew I, Fasulo D, Flanigan M, Florea L, Halpern A, Hannenhalli S, Kravitz S, Levy S, Mobarry C, Reinert K, Remington K, Abu-Threideh J, Beasley E, Biddick K, Bonazzi V, Brandon R, Cargill M, Chandramouliswaran I, Charlab R, Chaturvedi K, Deng Z, Di Francesco V, Dunn P, Eilbeck K, Evangelista C, Gabrielian AE, Gan W, Ge W, Gong F, Gu Z, Guan P, Heiman TJ, Higgins ME, Ji RR, Ke Z, Ketchum KA, Lai Z, Lei Y, Li Z, Li J, Liang Y, Lin X, Lu F, Merkulov GV, Milshina N, Moore HM, Naik

AK, Narayan VA, Neelam B, Nusskern D, Rusch DB, Salzberg S, Shao W, Shue B, Sun J, Wang Z, Wang A, Wang X, Wang J, Wei M, Wides R, Xiao C, Yan C, et al. 2001 The sequence of the human genome. Science **291**(5507)**:**1304-51.

68.   Risch N, Merikangas K 1996 The future of genetic studies of complex human diseases. Science **273:**1516-1517.

Category: Molecular Diagnostics and Genetics

Running head: GC Clamps for DHPLC

UTILITY OF GC CLAMPS IN MUTATION DETECTION BY DENATURING HIGH PERFORMANCE LIQUID CHROMATOGRAPHY

Robert J. Wurzburger[1]

Rajarsi Gupta[1]

Andrew P. Parnassa[1]

Sargam Jain[1]

Jason A. Wexler[1]

Jia Li Chu[1]

Paul Fogle[2]

Keith B. Elkon[1]

Robert D. Blank[1]

1. Research Division, The Hospital for Special Surgery, 535 East 70th St., New York, NY 10021

2. Transgenomic, Inc., 5600 South 42nd St., Omaha, NE 68107

Correspondence to RD Blank at the above address

Phone: (212) 606-1336

Fax: (212) 774-2739

e-mail: rdblank@mail.med.cornell.edu

ABSTRACT

Background: Enumeration of general principles for assay design using denaturing high performance liquid chromatography (DHPLC) would greatly facilitate the process of scanning genes for sequence variants.

Methods: Three target sequences harboring known allelic variants were studied to develop a general DHPLC assay design strategy. These were exon 10 of the human *RET* gene, exon 52 of the mouse *Cola2* gene, and exon 9 of the human *FAS* gene. Wavemaker v.3.3.3 software was used to analyze melting curves and determine assay conditions. GC clamps were added to PCR primers to introduce a high T_m domain to each of the target molecules. DHPLC was performed under partially denaturing conditions using the WAVE DNA fragment analysis system.

Results: DHPLC assays of PCR-amplified sequences can be developed at the computer by the following three simple steps. First, the target sequence should have a uniform T_m. Second, GC clamps of length sufficient to introduce a second melting domain with a $T_m \geq 8°$ above that of the target sequence should be appended to one of the primers. Third, the DHPLC assay should be performed at the highest temperature at which the molecule is predicted to be $\geq 90\%$ double stranded.

Conclusions: Assay design principles adapted from those previously established for denaturing gradient gel electrophoresis (DGGE) facilitate development of DHPLC mutation scanning strategies, as both methods resolve sequence variants by virtue of differences in the melting behavior of partially denatured DNA molecules. Use of GC clamps in DHPLC obviates the need for empirical optimization of new assays.

INTRODUCTION

Efficient, robust mutation detection methods can potentially have a major impact on the diagnosis of genetic disorders and the identification of genetic contributions to multifactorial disorders. Many investigations depend on relating genotypic variations to specific phenotypes. Scenarios in which this approach is potentially useful abound. Examples include searching for mutations of established pathogenic genes in specific syndromes (*e.g.* (1-3)), searching for mutations in candidate disease genes (*e.g.* (1)), searching for mutations in positional candidates for disease loci (*e.g.* (2-4)), and searching for polymorphisms that predispose to multifactorial disorders or traits (*e.g.* (5, 6)).

Such assays should ideally possess several performance characteristics (reviewed by (7, 8)). They should be sensitive and specific. They should allow easy incorporation of positive and negative controls to allow assay performance to be monitored over time. They must require a minimum of operator and instrument time. Finally, they should be based on principles that are well understood so that new assays can easily be developed. This last feature is particularly important for genetic tests since any single test assays only a minuscule fraction of the genome.

Other than sequence determination, most mutation detection strategies can be grouped into four categories. The first are hybridization-dependent and include allele-specific hybridization (*e.g.* (9)), allele-specific amplification (*e.g.* (10, 11)), and solid-phase resequencing (*e.g.* (12)). These methods can be used without electrophoresis, making them attractive for high-throughput applications. They are limited by requiring separate assays to be designed for each potential mutation. The second are conformation-dependent and include single stranded conformational polymorphism (SSCP) (13) and conformation sensitive gel electrophoresis (CSGE) (14, 15). These methods are easily performed but are limited in sensitivity unless

carefully optimized or run under multiple conditions and require electrophoresis. The third are cleavage-based methods in which either an enzymatic or chemical cleavage occurs at the positions of strand mismatches in heteroduplex DNA molecules (*e.g.* (16-19)). These methods have the advantage of localizing mutations as well as detecting their presence. They are limited insofar as they are relatively demanding technically. The fourth are melting-dependent and include denaturing gradient gel electrophoresis (DGGE) (20), DGGE derivatives (21-23), and denaturing high performance liquid chromatography (DHPLC) (24). These methods are extremely sensitive but require significant effort to design each assay. Moreover, all except DHPLC require electrophoresis, limiting throughput.

In this report, we describe a simplified strategy for designing mutation detection assays using the WAVE DNA fragment analysis system, an integrated, semi-automated DHPLC apparatus. The strategy is based on the dependence of both DHPLC and DGGE on resolving partially denatured double stranded DNA molecules. Particular attention is devoted to the use of GC clamps with this system, allowing assay design to be carried out in a nearly algorithmic fashion. This approach allows investigators to shift their efforts from mutation detection assay design to interpretation of the biological consequences of detected sequence variation.

MATERIALS AND METHODS

DNA preparation: Mouse DNA was prepared from 2-3 mm of tail using the Invitrogen (Carlsbad, CA) DNA extraction kit. Human DNA was prepared from peripheral blood mononuclear cells using the Puregene (Minneapolis, MN) DNA extraction kit. Human subjects provided written informed consent under protocols approved by the Memorial Sloan-Kettering Cancer Center's IRB (25, 26) or the Hospital for Special Surgery's IRB ((27-29)).

Choice of Polymerase Chain Reaction (PCR) targets: The DNA sequence to be scanned for

mutations was entered into the interactive window in WAVEMAKER (version 3.3.3) software (Transgenomic, Inc., Omaha, NE). The target must include sufficient flanking sequence so that primers in which mutations will not be sought can be designed. WAVEMAKER displays a position v T_m plot that allows determination of the range of temperatures over which the sequence denatures. Appropriate targets have uniform melting temperatures along the length of the sequence except for lower-melting regions at either end. If the proposed target sequence includes regions with melting temperatures differing by more than 2 to 3°C, then these should be amplified and analyzed separately.

PCR: All amplifications were performed in 50 µl reactions including 1 U of Red Taq DNA Polymerase (Sigma, St. Louis, MO), 0.2 mM dNTP mix (Amersham Pharmacia, Piscataway, NJ), and 10 mM Tris-HCl (pH 8.3) containing 50 mM KCl, 1.5 mM $MgCl_2$, 0.1% gelatin, and 20 - 50 ng of genomic DNA. Primers were designed using Primer 0.5 software (30). Primer sequences and annealing temperatures are given in Table 1. Reactions were performed in a PE Biosystems (Norwalk, CT) 2400 thermal cycler. Amplifications were carried out by an initial denaturation of 3 minutes at 95°C followed by 35 cycles of 94° C X 30 seconds, $T_{annealing}$ X 30 seconds, and 72° C X 30 seconds. Following amplification, samples were subjected to a final denaturation at 95° C X 5 minutes followed by slow cooling to room temperature.

DHPLC conditions: Loading, elution, and washing of the DHPLC column was carried out with varying combinations of 3 buffers. Buffer A contains 100 mM triethylamine acetate (TEAA), pH 7.0 and 0.025% acetonitrile, buffer B contains 25% acetonitrile, 100 mM TEAA, pH 7.0, and 0.1 mM EDTA, and buffer D contains 75% acetonitrile. DHPLC elution buffer gradients were generated by WAVEMAKER version 3.3.3 software. Assays were performed using the Transgenomic, Inc. WAVE DNA fragment analysis system. Oven temperature was determined

from inspection of the melting profile, choosing the highest temperature at which the target sequence was predicted to be >90% duplex. Following the gradient elution, all remaining bound material was washed from the column with buffer D. Sample elution was monitored by absorbance at 260 nm.

DNA Sequencing: PCR products were purified by passage through Microcon microconcentrating centrifugal filter columns (Millipore, Bedford, MA) prior to sequencing. Sequencing reactions were performed using the PE Biosystems Dye-Terminator Kit and analyzed on a PE Biosystems 377 DNA sequencer.

RESULTS

Since both DGGE and DHPLC-based mutation detection operate on the principle of detecting differences in melting behavior among individual species in a mixed population of DNA molecules, we first adapted an established DGGE assay to performance on the WAVE instrument.

Exon 10 of the *RET* protooncogene was chosen for this experiment. Point mutations of various cysteine residues of exons 10 and 11 of this gene lead to multiple endocrine neoplasia type 2 A or familial medullary carcinoma of the thyroid (31, 32). We previously developed DGGE assays to detect pathogenic mutations in exon 10 (25, 26). The *RET* exon 10 sequence was entered into WAVEMAKER with and without the 36 bp GC clamp sequence. The melting profile of the target sequence was predicted and verified to be uniform within the target region. Without the GC clamp, there is a single melting domain, with 'breathing' at the ends of the molecule. Addition of the GC clamp introduces a second higher T_m melting domain (Figure 1). The target sequence therefore denatures under conditions in which the GC clamp remains double-stranded. The melting curves generated by WAVEMAKER demonstrated that the target

sequence would be completely double stranded at 65°C, >90% double stranded at 66° C, and ~20% double stranded at 67°C (Figure 2). WAVEMAKER also generated a gradient profile (Table 2). We used the temperature from inspection of the melting curve rather than that picked by WAVEMAKER to perform the assay, as WAVEMAKER does not distinguish between the target sequence and the higher T_m GC clamp. WAVEMAKER's temperature is generally 1°C higher than that obtained by manual inspection of the melting curve. *RET* exon 10 was amplified from subjects harboring the C620F and C620R mutations, suffering from familial medullary carcinoma of the thyroid and MEN 2A, respectively, and from unaffected family members (26). Mutations were detected at 66°C (figure 3), 67°C (not shown), but not at 65°C or 68°C (not shown) when the GC clamp was included. These mutations were resolved at 60°C using a 20-60% gradient by DGGE (25). Mutations were not detected either by DHPLC or DGGE when the GC clamp was not used (not shown).

We next designed a mutation detection assay for the mouse $Cola2^{oim}$ mutation. This mutation is a 1 bp deletion of a G residue in the C-terminal propeptide of the gene encoding the α2 chain of type 1 procollagen (33, 34). Mice harboring either one or two mutant alleles display varying degrees of skeletal fragility compared to their wild-type littermates (33, 35). The degree of skeletal fragility is determined by homo- or heterozygosity for the mutant allele and by segregation of background genes in the system (35, 36) (Camacho, unpublished data; Blank unpublished data). This mutation is not detectable by a restriction enzyme recognition site polymorphism and thus far, genotyping animals for the mutation has depended either on direct sequencing or an allele-specific amplification (37, 38).

We developed a DHPLC assay to detect this mutation following the strategy used for *RET* exon 10. The melting profile of the *Cola2* exon 52 was determined in WAVEMAKER and

determined to be uniform in the target region (Figure 4a). The target sequence is > 90% double stranded at 58°C but not at 59°C (Figure 4b). Gradient conditions were those provided by WAVEMAKER (Table 3). Oven temperature was chosen to be 58°C based on the melting curves shown in Figure 4b. Heterozygotes were readily distinguished from either wild-type or mutant homozygotes when a 36 bp GC clamp was included (Figure 4c), but not when it was omitted (not shown). Mutations were not detected at 59°C (not shown), the temperature chosen by WAVEMAKER. A 50:50 mix of wild-type and mutant homozygous samples eluted as a single sharp peak when unheated, but eluted as a pair of peaks when heated to 95°C and cooled slowly (Figure 4d). These data demonstrate that these assay conditions are robust for determining heterozygosity at the *Cola2* locus, but are not adequate for determining the allele present in homozygous samples. Moreover, the behavior of the unheated mixture reveals that there is no difference in the elution times of the wild-type and mutant products, as the peak is not broadened relative to the peak generated by homozygous samples. Thus, the sensitivity of mutation detection is greater in the setting of heterozygosis than homozygosis. This finding indicates that decreased T_m at the site of mismatch is a critical element of mutation detection by DHPLC.

Homozygous samples can be genotyped in a two-step assay. In the first step, the assay is performed on a pure sample. In the second step, samples found to be homozygous are mixed with a reference wild-type sample, denatured, reannealed and reanalyzed. Mutant homozygotes will yield a heterozygous pattern on mixing while wild-type homozygotes will retain a homozygous pattern on mixing.

We applied our strategy for mutation detection to the human *FAS* (*APO-1*, *CD95*) gene. Mutations of this gene cause the Canale-Smith Syndrome, a disease characterized by

hypergammaglobulinemia, systemic autoimmunity, lymphadenopathy and splenomegaly (27, 39). We previously identified mutations in 14 probands with this disorder, and patients heterozygous for an A to G change at cDNA nucleotide 913 resulting in D244G and a G to C change at cDNA nucleotide 883 resulting in R234P missense mutations were studied here (27, 29). These patients each suffered the typical clinical features of the syndrome as previously described (patients 7 and 8, respectively of (29)).

DHPLC analysis of these patients and an unaffected sib of one of them are summarized in Table 4 and Figure 5. As we observed for *RET* and *Cola2*, the mutations were readily detected with a GC clamp at the temperature predicted to be optimal by inspection of the melting curve. Again as observed for the other assays, omission of the GC clamps did not allow us to detect the mutations (not shown).

DISCUSSION

Heteroduplexes include mismatches of one or more base pairs, resulting in early melting of the mismatched region. DHPLC allows resolution of heteroduplex from homoduplex DNA molecules based on differences in their retention time in the column under partially denaturing conditions, with heteroduplex molecules eluting earlier. This behavior mirrors heteroduplexes' lower T_m's and is similar to retardation of electrophoretic transport at different points along a denaturing gradient gel. In DGGE, mutations in the highest T_m domain are resolved poorly, if at all. We reasoned that while the analytical technology differs in DHPLC, the principle of heteroduplex detection should be the same as in DGGE and that inclusion of GC clamps would facilitate mutation detection. The inability to detect sequence variants in the highest T_m domain may explain the anecdotally poor ability of DHPLC to detect mutations in short amplicons (K. Hecker, personal communication), which often include only a single melting domain.

We have established a simple and general approach to designing new mutation screening assays by DHPLC. First, the target region's sequence is entered into WAVEMAKER or an equivalent melting analysis program and assessed for uniformity of T_m. If this condition is not satisfied, alternative primers that allow for a uniform T_m are chosen. Next, a GC clamp of sufficient length to create a high-T_m domain is appended to one of the primers. Melting curves of the PCR product are calculated and the highest temperature at which the target sequence is >90% duplex is chosen for assay performance. WAVEMAKER determined elution conditions are used.

The trio of assays described here demonstrate that inclusion of a GC clamp allows detection of mutations by DHPLC under conditions that can be fully established prior to assay performance, using the melting curves generated by WAVEMAKER. The experiments presented above do not exclude the development of assays without GC clamps, but rather show that the conditions identified by WAVEMAKER work well without further optimization when GC clamps are included.

Sheffield and colleagues demonstrated the utility of GC clamps in designing DGGE assays (40), showing that the inclusion of a clamp allowed detection of mutations in the murine β^{major} globin gene that were undetectable without clamping. The additional sensitivity arose from detection of mutations in the highest T_m domain of the target sequence. Subsequent sensitivity analyses of DGGE have consistently found that analyses performed with GC clamps have sensitivities of ~95% and specificities approaching unity (e.g. (41-44)). The theoretical basis for this increase in sensitivity is that resolution of the various molecular species present occurs primarily when the individual molecules are partially denatured. Inclusion of a GC clamp provides an artificial, high T_m domain into the molecules being analyzed, allowing the target

sequence to occur in the context of a low T_m domain. Our data suggest that resolution of the various molecular species by DHPLC also occurs primarily when these have partially denatured, so that the principles guiding design of DGGE assays can be applied to DHPLC mutation detection.

In the assays described here, the GC clamp had a melting point 8-13°C higher than the target sequence, while the target sequence varied in T_m by no more than 3°C. We therefore suggest that investigators include GC clamp sequences sufficiently long to provide an 8°C increment in Tm relative to the target. The required length will vary according to the T_m of the target sequence.

Theoretically, psoralen clamping provides an alternative to GC clamping by generating a covalent interstrand bond rather than by raising the T_m of a region of the target molecule (45). The covalent bond introduced by psoralenation and subsequent UV light exposure effectively clamps one end of the molecule regardless of temperature. The advantage of psoralen compared to GC clamping is that the clamp need not be changed from assay to assay; the disadvantage is that an additional UV crosslinking step must be added prior to analysis. However, we have not conducted any experiments with psoralen clamps and cannot comment on whether this approach would perform as well in practice as in theory.

Electrophoretic mutation detection assays are difficult to perform on a large scale, since casting and loading gels are tasks that are difficult to automate. Because DGGE and SSCP suffer from these limitations, the DHPLC-based assay is more readily adaptable to a high-throughput setting. The WAVE system can load samples automatically from a 96-sample block and process each sample in approximately 6 to 9 minutes. This allows investigators to perform mutation screens at higher throughput and with less hands-on time than would be possible by gel-based

methods. Further improvements in throughput might be achieved by pooling samples prior to DHPLC analysis, as has been done for gel-based methods (*e.g.* (46)).

High sensitivity and specificity have been reported for DHPLC in a growing body of analyses (e.g. (47-53)). These reports document that carefully performed DHPLC equals or surpasses other mutation screening methods' accuracy.

The greatest limitation on throughput, however, remains the time necessary to design mutation detection assays. To our knowledge, only one previous report addressed assay design optimization (54). These authors recommended performing assays at the T_m determined by the melting analysis program DHPLCMelt and 2°C above that temperature. We have demonstrated that inclusion of GC clamps obviates the need for tedious assay optimization. GC clamps of a length sufficient to create a domain with T_m 8°C greater than that of the target sequence allows an experimenter to develop a working assay in less than one hour. As genomic analysis moves from determination of additional sequence data to understanding the biological consequences of sequence variation, the ability to perform mutation screening efficiently will become ever more valuable. The WAVEMAKER based algorithm for establishing DHPLC conditions described here will facilitate this.

ACKNOWLEDGMENTS

REFERENCES

1. Buchner G, Orfanelli U, Quaderi N, Bassi MT, Andolfi G, Ballabio A, et al. Identification of a new EGF-repeat-containing gene from human xp22: A candidate for developmental disorders. Genomics 2000;65:16-23.

2. Giampietro PF, Raggio CL and Blank RD. Synteny-defined candidate genes for congenital and idiopathic scoliosis. Am J Med Genet 1999;83:164-77.

3. Turnpenny PD, Bulman MP, Frayling TM, Abu-Nasra TK, Garrett C, Hattersley AT, et al. A gene for autosomal recessive spondylocostal dysostosis maps to 19q13.1-q13.3. Am J Hum Genet 1999;65:175-82.

4. Bulman MP, Kusumi K, Frayling TM, McKeown C, Garrett C, Lander ES, et al. Mutations in the human delta homologue, DLL3, cause axial skeletal defects in spondylocostal dysostosis. Nat Genet 2000;24:438-41.

5. Zmuda JM, Cauley JA and Ferrell RE. Recent progress in understanding the genetic susceptibility to osteoporosis. Genet Epidemiol 1999;16:356-67.

6. Giguere Y and Rousseau F. The genetics of osteoporosis: 'complexities and difficulties' . Clin Genet 2000;57:161-9.

7. Grompe M. The rapid detection of unknown mutations in nucleic acids. Nature Genet. 1993;5:111-117.

8. Cotton RG. Slowly but surely towards better scanning for mutations. Trends Genet 1997;13:43-6.

9. Kazazian HH, Jr., Orkin SH, Markham AF, Chapman CR, Youssoufian H and Waber PG. Quantification of the close association between DNA haplotypes and specific beta-thalassaemia mutations in Mediterraneans. Nature 1984;310:152-4.

10. Wu DY, Ugozzoli L, Pal BK and Wallace RB. Allele-specific enzymatic amplification of beta-globin genomic DNA for diagnosis of sickle cell anemia. Proc Natl Acad Sci U S A 1989;86:2757-60.

11. Barany F. Genetic disease detection and DNA amplification using cloned thermostable ligase. Proc Natl Acad Sci U S A 1991;88:189-93.

12. Gunderson KL, Huang XC, Morris MS, Lipshutz RJ, Lockhart DJ and Chee MS. Mutation detection by ligation to complete n-mer DNA arrays. Genome Res 1998;8:1142-53.

13. Orita M, Iwahana H, Kanazawa H, Hayashi K and Sekiya T. Detection of polymorphisms of human DNA by gel electrophoresis as single-strand conformation polymorphisms. Proc Natl Acad Sci U S A 1989;86:2766-70.

14. Ganguly A, Rock MJ and Prockop DJ. Conformation-sensitive gel electrophoresis for rapid detection of single-base differences in double-stranded PCR products and DNA fragments: evidence for solvent-induced bends in DNA heteroduplexes. Proc Natl Acad Sci U S A 1993;90:10325-9.

15. Korkko J, Annunen S, Pihlajamaa T, Prockop DJ and Ala-Kokko L. Conformation sensitive gel electrophoresis for simple and accurate detection of mutations: comparison with denaturing gradient gel electrophoresis and nucleotide sequencing. Proc Natl Acad Sci U S A 1998;95:1681-5.

16. Cotton RG, Rodrigues NR and Campbell RD. Reactivity of cytosine and thymine in single-base-pair mismatches with hydroxylamine and osmium tetroxide and its application to the study of mutations. Proc Natl Acad Sci U S A 1988;85:4397-401.

17. Gogos JA, Karayiorgou M, Aburatani H and Kafatos FC. Detection of single base mismatches of thymine and cytosine residues by potassium permanganate and hydroxylamine in

the presence of tetralkylammonium salts. Nucleic Acids Res 1990;18:6807-14.

18. Youil R, Kemper BW and Cotton RG. Screening for mutations by enzyme mismatch cleavage with T4 endonuclease VII. Proc Natl Acad Sci U S A 1995;92:87-91.

19. Fox KR, Allinson SL, Sahagun-Krause H and Brown T. Recognition of GT mismatches by Vsr mismatch endonuclease. Nucleic Acids Res 2000;28:2535-40.

20. Myers RM, Maniatis T and Lerman L. Denaturing gradient gel electrophoresis. Methods in Enzymology 1987;155:501-527.

21. Borresen AL, Hovig E, Smith-Sorensen B, Malkin D, Lystad S, Andersen TI, et al. Constant denaturant gel electrophoresis as a rapid screening technique for p53 mutations. Proc Natl Acad Sci U S A 1991;88:8405-9.

22. Yoshino K, Nishigaki K and Husimi Y. Temperature sweep gel electrophoresis: a simple method to detect point mutations. Nucleic Acids Res 1991;19:3153.

23. Henco K, Harders J, Wiese U and Riesner D. Temperature gradient gel electrophoresis (TGGE) for the detection of polymorphic DNA and RNA. Methods Mol Biol 1994;31:211-28.

24. Oefner PJ and Underhill PA. (2000) DNA Mutation Detection Using Denaturing High-Performance Liquid Chromatography (DHPLC). Current Protocols in Human Genetics. Unit 7.10.

25. Blank RD, Sklar CA and Martin ML. Denaturing gradient gel electrophoresis to diagnose multiple endocrine neoplasia type 2. Clin Chem 1996;42:598-603.

26. Blank RD, Sklar CA, Dimich AB, LaQuaglia MP and Brennan MF. Clinical presentations and RET protooncogene mutations in seven multiple endocrine neoplasia type 2 kindreds. Cancer 1996;78:1996-2003.

27. Drappa J, Vaishnaw AK, Sullivan KE, Chu JL and Elkon KB. Fas gene mutations in the

Canale-Smith syndrome, an inherited lymphoproliferative disorder associated with autoimmunity. N Engl J Med 1996;335:1643-9.

28. Vaishnaw AK, Toubi E, Ohsako S, Drappa J, Buys S, Estrada J, et al. The spectrum of apoptotic defects and clinical manifestations, including systemic lupus erythematosus, in humans with CD95 (Fas/APO-1) mutations. Arthritis Rheum 1999;42:1833-42.

29. Vaishnaw AK, Orlinick JR, Chu JL, Krammer PH, Chao MV and Elkon KB. The molecular basis for apoptotic defects in patients with CD95 (Fas/Apo-1) mutations.   J Clin Invest 1999;103:355-63.

30. Lincoln SE, Daly MJ and Lander ES. (1991) Primer: a computer program for automatically selecting PCR primers.

31. Donis-Keller H, Dou S, Chi D, Carlson KM, Toshima K, Lairmore TC, et al. Mutations in the RET proto-oncogene are associated with MEN 2A and FMTC.   Hum. Mol. Genet. 1993;2:851-856.

32. Mulligan LM, Kwok JBJ, Healey CS, Elsdon MJ, Eng C, Gardner E, et al. Germ-line mutations of the RET proto-oncogene in multiple endocrine neoplasia type 2A.   Nature 1993;363:458-460.

33. Chipman SD, Sweet HO, McBride DJJ, Davisson MT, Marks SCJ, Shuldiner AR, et al. Defective proα2(I) collagen synthesis in a recessive mutation in mice: a model of human osteogenesis imperfecta. Proc Natl Acad Sci USA 1993;90:1701-1705.

34. McBride DJ, Jr. and Shapiro JR. Confirmation of a G nucleotide deletion in the Cola-2 gene of mice with the osteogenesis imperfecta mutation. Genomics 1994;20:135-7.

35. Saban J, Zussman MA, Havey R, Patwardhan AG, Schneider GB and King D. Heterozygous oim mice exhibit a mild form of osteogenesis imperfecta. Bone 1996;19:575-9.

36. McBride DJ, Jr., Shapiro JR and Dunn MG. Bone geometry and strength measurements in aging mice with the oim mutation. Calcif Tissue Int 1998;62:172-6.

37. Camacho NP, Dow D, Toledano TR, Buckmeyer JK, Gertner JM, Brayton CF, et al. Identification of the oim mutation by dye terminator chemistry combined with automated direct DNA sequencing. J Orthop Res 1998;16:38-42.

38. Saban J and King D. PCR genotyping of oim mutant mice. Biotechniques 1996;21:190, 192.

39. Fisher GH, Rosenberg FJ, Straus SE, Dale JK, Middleton LA, Lin AY, et al. Dominant interfering Fas gene mutations impair apoptosis in a human autoimmune lymphoproliferative syndrome. Cell 1995;81:935-46.

40. Sheffield VC, Cox DR, Lerman LS and Myers RM. Attachment of a 40-base-pair G+C-rich sequence (GC-clamp) to genomic DNA fragments by the polymerase chain reaction results in improved detection of single-base changes. Proc. Natl. Acad. Sci. USA 1989;86:232-236.

41. Guldberg P, Henriksen KF and Guttler F. Molecular analysis of phenylketonuria in Denmark: 99% of the mutations detected by denaturing gradient gel electrophoresis. Genomics 1993;17:141-6.

42. Nissen H, Petersen NE, Mustajoki S, Hansen TS, Mustajoki P, Kauppinen R, et al. Diagnostic strategy, genetic diagnosis and identification of new mutations in intermittent porphyria by denaturing gradient gel electrophoresis. Hum Mutat 1997;9:122-30.

43. Macek M, Jr., Mercier B, Mackova A, Miller PW, Hamosh A, Ferec C, et al. Sensitivity of the denaturing gradient gel electrophoresis technique in detection of known mutations and novel Asian mutations in the CFTR gene. Hum Mutat 1997;9:136-47.

44. Gejman PV, Cao Q, Guedj F and Sommer S. The sensitivity of denaturing gradient gel

electrophoresis: a blinded analysis. Mutat Res 1998;382:109-14.

45. Costes B, Girodon E, Ghanem N, Chassignol M, Thuong NT, Dupret D, et al. Psoralen-modified oligonucleotide primers improve detection of mutations by denaturing gradient gel electrophoresis and provide an alternative to GC-clamping. Hum Mol Genet 1993;2:393-7.

46. Zarbl H, Aragaki C and Zhao LP. An efficient protocol for rare mutation genotyping in a large population. Genet Test 1998;2:315-21.

47. Liu WO, Oefner PJ, Qian C, Odom RS and Francke U. Denaturing HPLC-identified novel FBN1 mutations, polymorphisms, and sequence variants in Marfan syndrome and related connective tissue disorders. Genet Test 1997;1:237-42.

48. Liu W, Smith DI, Rechtzigel KJ, Thibodeau SN and James CD. Denaturing high performance liquid chromatography (DHPLC) used in the detection of germline and somatic mutations. Nucleic Acids Res 1998;26:1396-400.

49. O' Donovan M, Oefner PJ, Roberts SC, Austin J, Hoogendoorn B, Guy C, et al. Blind analysis of denaturing high-performance liquid chromatography as a tool for mutation detection. Genomics 1998;52:44-9.

50. Choy YS, Dabora SL, Hall F, Ramesh V, Niida Y, Franz D, et al. Superiority of denaturing high performance liquid chromatography over single-stranded conformation and conformation-sensitive gel electrophoresis for mutation detection in TSC2 . Ann Hum Genet 1999;63:383-91.

51. Gross E, Arnold N, Goette J, Schwarz-Boeger U and Kiechle M. A comparison of BRCA1 mutation analysis by direct sequencing, SSCP and DHPLC. Hum Genet 1999;105:72-8.

52. Wagner T, Stoppa-Lyonnet D, Fleischmann E, Muhr D, Pages S, Sandberg T, et al. Denaturing high-performance liquid chromatography detects reliably BRCA1 and BRCA2 mutations. Genomics 1999;62:369-76.

53. Dobson-Stone C, Cox RD, Lonie L, Southam L, Fraser M, Wise C, et al. Comparison of fluorescent single-strand conformation polymorphism analysis and denaturing high-performance liquid chromatography for detection of EXT1 and EXT2 mutations in hereditary multiple exostoses. Eur J Hum Genet 2000;8:24-32.

54. Jones AC, Austin J, Hansen N, Hoogendoorn B, Oefner PJ, Cheadle JP, et al. Optimal temperature selection for mutation detection by denaturing HPLC and comparison to single-stranded conformation polymorphism and heteroduplex analysis. Clin Chem 1999;45:1133-40.

Table 1. PCR Primers and Annealing Temperatures

Primer ID	Primer Sequence	$T_{annealing}$	Reference
FRET10	GCGCCCCAGGAGGCTGAGTG	65°	(31)
RRET10	CGTGGTGGTCCCGGCCGCC		(31)
RRET10c	Clamp36-CGTGGTGGTCCCGGCCGCC		(25)
FOIM	GAAATGGCTTTCCTAGACCCCG	60°	this study
ROIM	AATGATTGTCTTGCCCCATTCA		this study
ROIMc	Clamp36-AATGATTGTCTTGCCCCATTCA		this study
HFAS49	ATGTTGACTTGAGTAAATAT	55°C	(27)
HFAS47	CTTTCCATGAAGTTGATGCC		(27)
HFAS49c	Clamp20-ATGTTGACTTGAGTAAATAT		this study
Clamp20	GCGGCCCGCCGCCCCGCCG		
Clamp36	CGCCCGCCGCGCCCCGCGCCCGTCCCGCCGCCCCGCCCCG		(40)

Table 2. Assay Conditions for *RET10*

Oven Temperature = 66°C, Flow Rate = 0.9 ml/min

Time	%A	%B	%D
0.0	56	44	0
0.5	51	49	0
5.0	42	58	0
5.1	0	0	100
5.6	0	0	100
5.7	56	44	0
8.2	56	44	0

Table 3. Assay Conditions for *Cola2*

Oven Temperature = 58°C, Flow Rate = 0.9 ml/min

Time	%A	%B	%D
0.0	57	43	0
0.5	52	48	0
5.0	43	57	0
5.1	0	0	100
5.6	0	0	100
5.7	57	43	0
8.2	57	43	0

Table 4. Assay Conditions for *Fas*

Oven Temperature = 59°C, Flow Rate = 0.9 ml/min

Time	%A	%B	%D
0.0	55	45	0
0.5	50	50	0
5.0	41	59	0
5.1	0	0	100
5.6	0	0	100
5.7	55	45	0
8.2	55	45	0

FIGURE LEGENDS

Figure 1. Melting profiles for *RET10* without (top) and with (bottom) inclusion of a 36 base GC clamp on the 3' amplification primer. The bold lines under the base-pair axis indicate the extent of the primer sequences.

Figure 2. Predicted melting behavior of GC clamped *RET10* amplicons at $65°$, $66°$, and $67°$. The GC clamp remains double stranded at all 3 temperatures. The target sequence is $\geq 90\%$ double stranded at $65°$ and $66°$, but not at $67°$.

Figure 3. DHPLC elution profiles for 3 *RET* genotypes at $66°$. Heterozygotes harboring the C620F and C620R mutations are readily distinguished from normals and from each other.

Figure 4. *Cola2* DHPLC assay. The GC clamped melting profile is shown in panel A. The predicted melting behavior of *Cola2* amplicons at $57°$, $58°$, and $59°$ are shown in panel B. Resolution of *Cola2* heterozygotes from homozygotes is shown in panel C. Inability to resolve +/+ homozygotes from *oim/oim* homozygotes is shown in panel D.

Figure 5. *FAS* DHPLC assay. The GC clamped melting profile is shown in panel A. The predicted melting behavior of *FAS* amplicons at $58°$, $59°$, and $60°$ are shown in panel B. Resolution of R234P and D244G heterozygotes from a wild-type homozygote is shown in panel C.

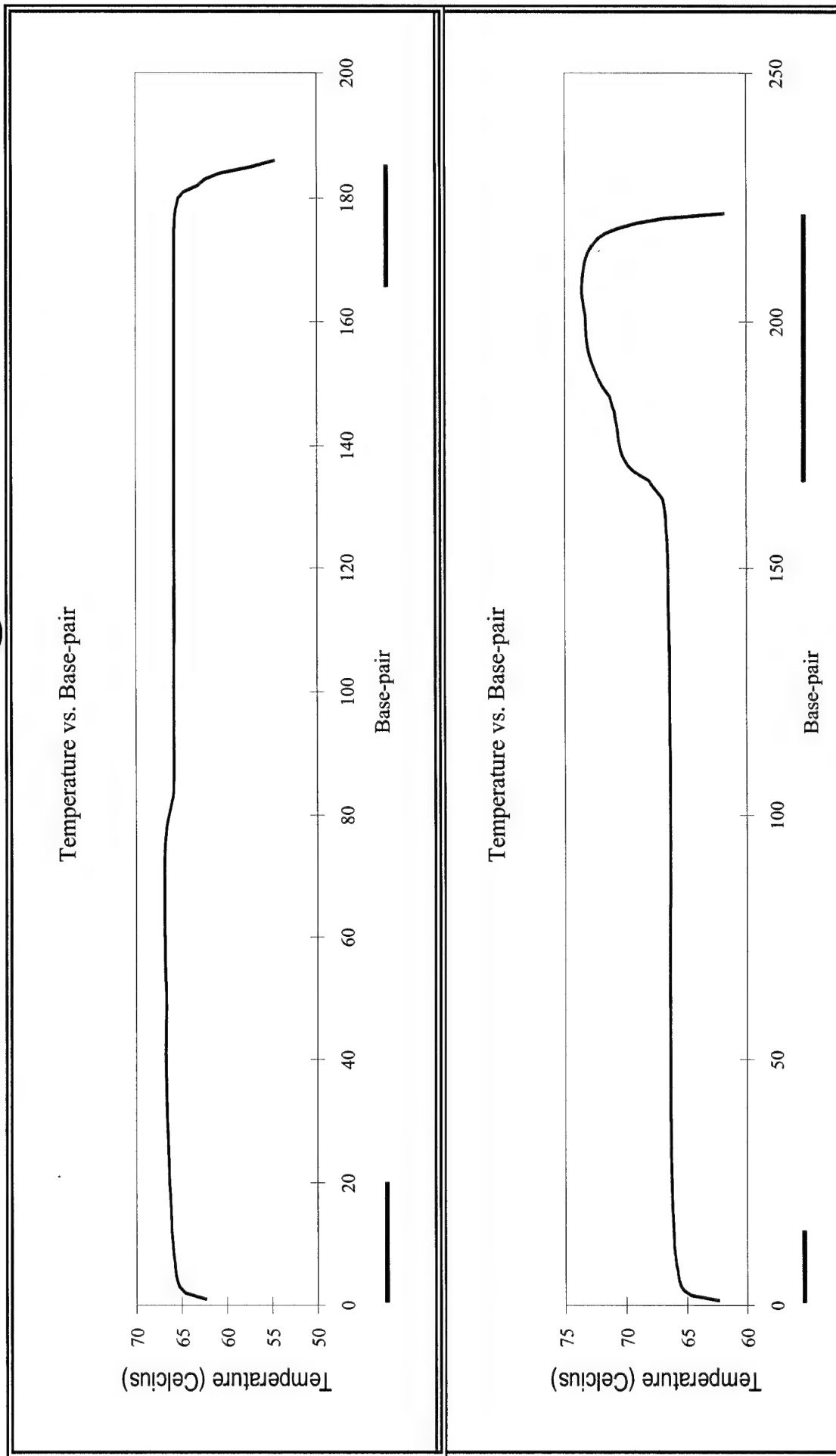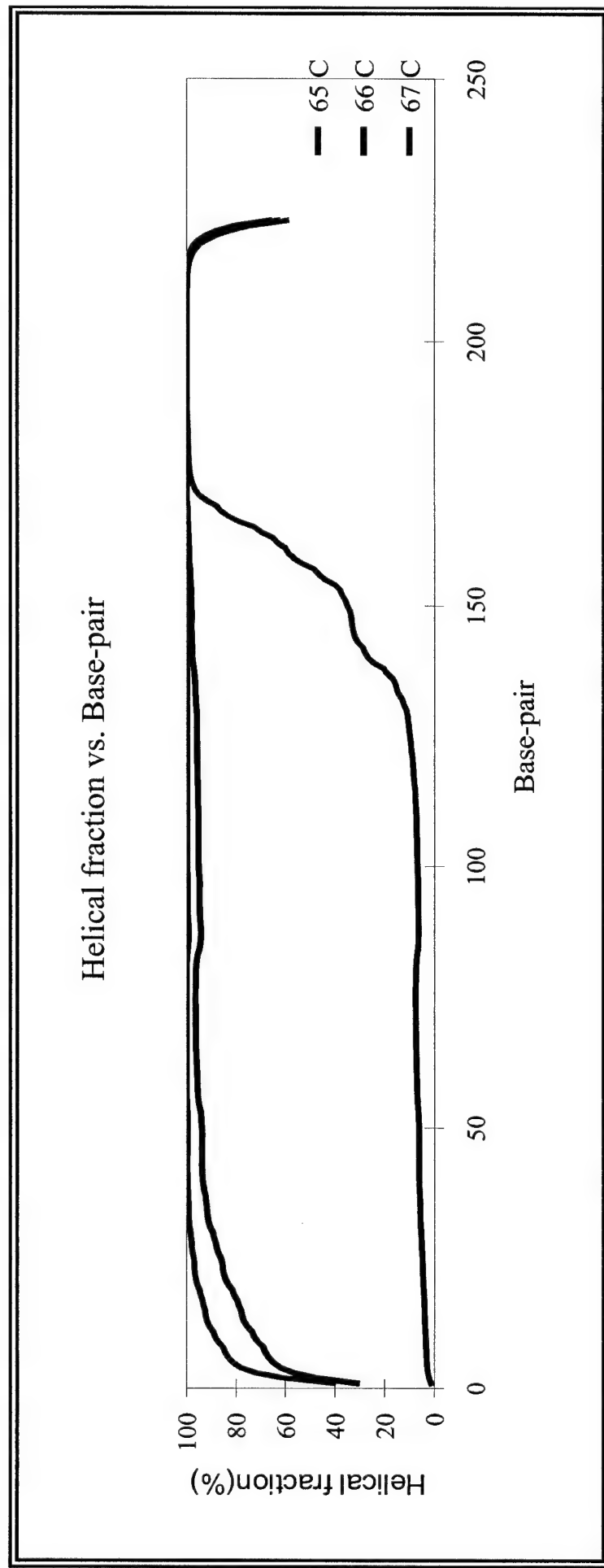# Figure 1

RET10 Melting Profiles

Temperature vs. Base-pair

Base-pair

Temperature vs. Base-pair

Base-pair

Figure 2

Temperature and *RET10* Melting

Helical fraction vs. Base-pair

Figure 3

RET Exon 10 Mutation Detection 66°C
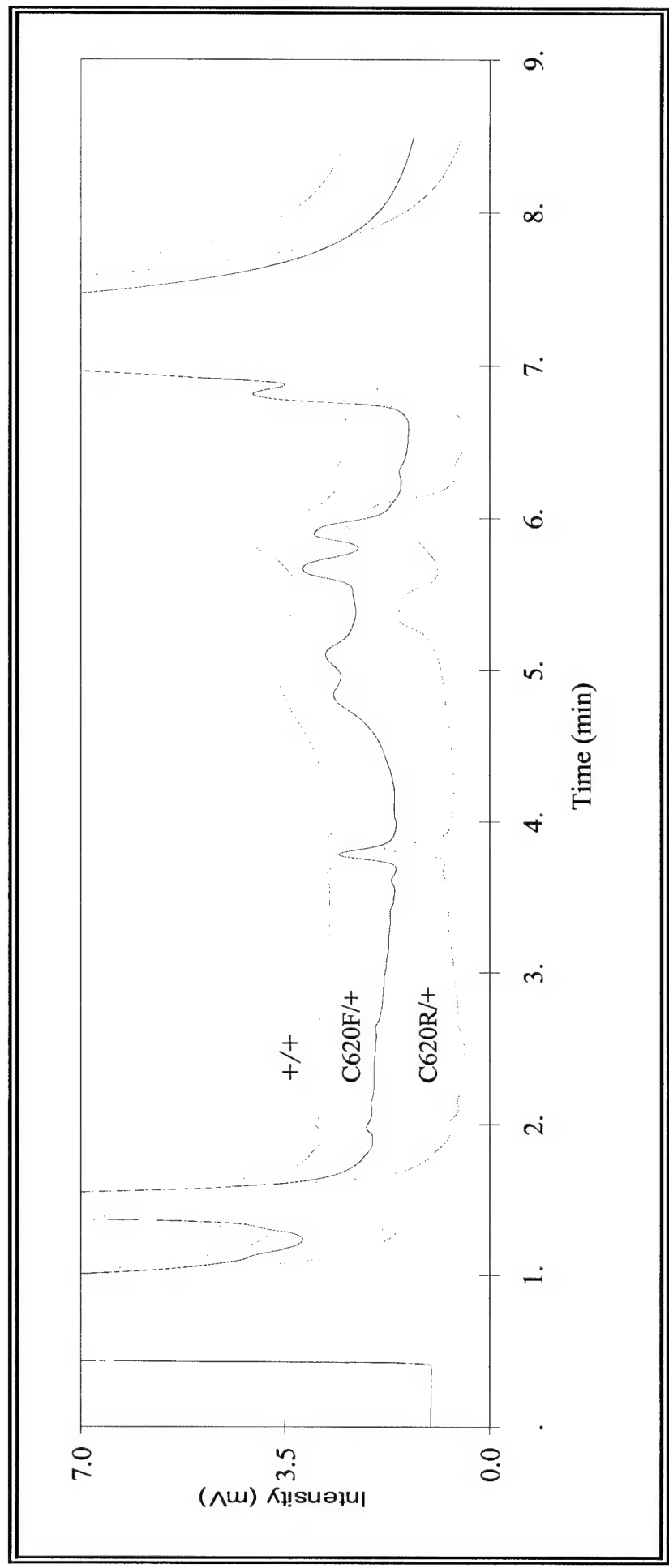
Figure 4A

Cola2 Melting Profile

Temperature vs. Base-pair
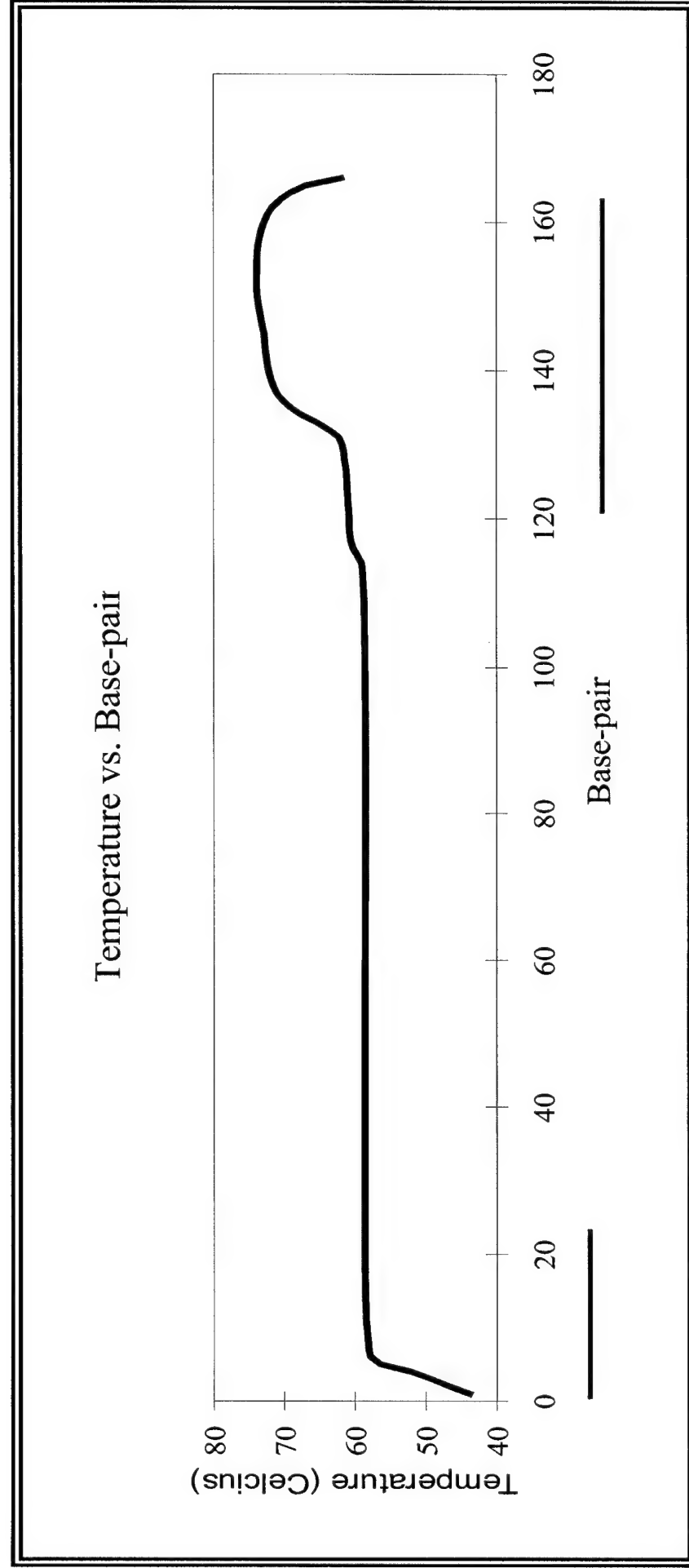
Figure 4B

Temperature and *Cola2* Melting

Helical fraction vs. Base-pair
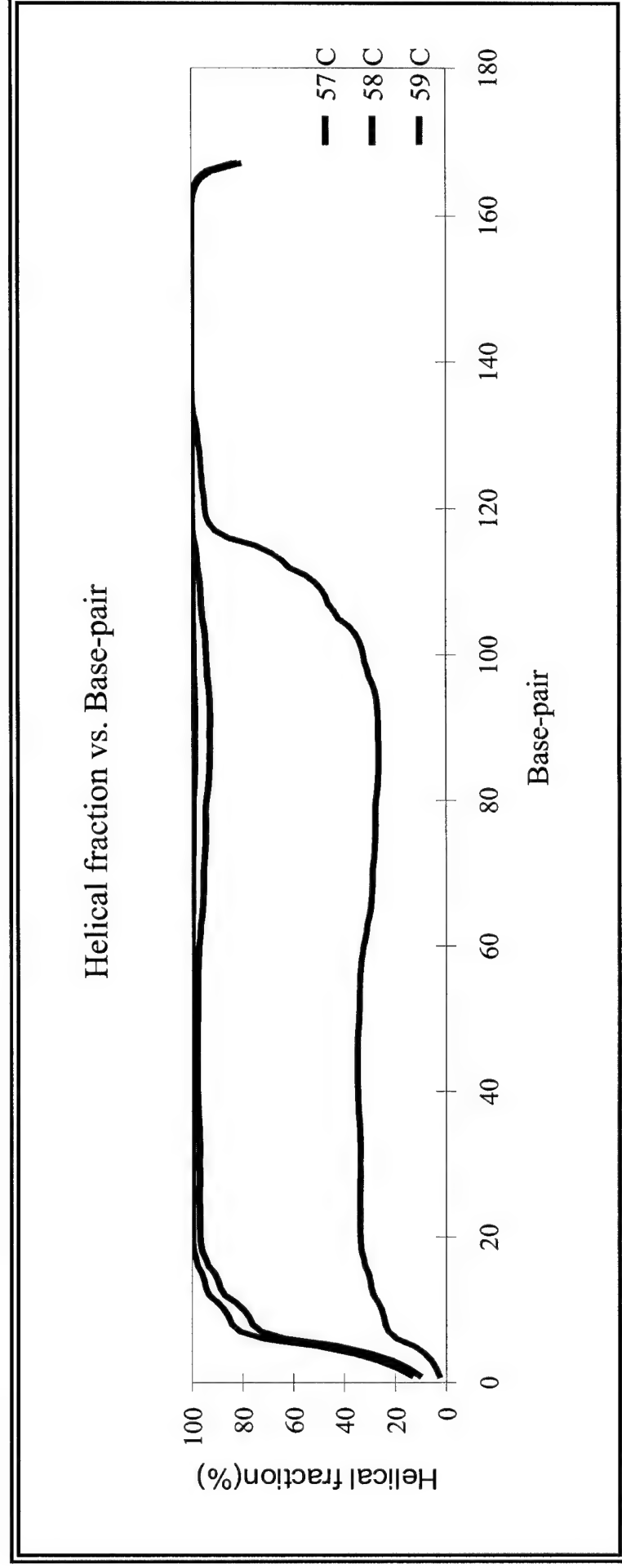
Helical fraction(%)

Base-pair

— 57 C
— 58 C
— 59 C

Figure 4C

Cola2 Mutation Detection 58°C
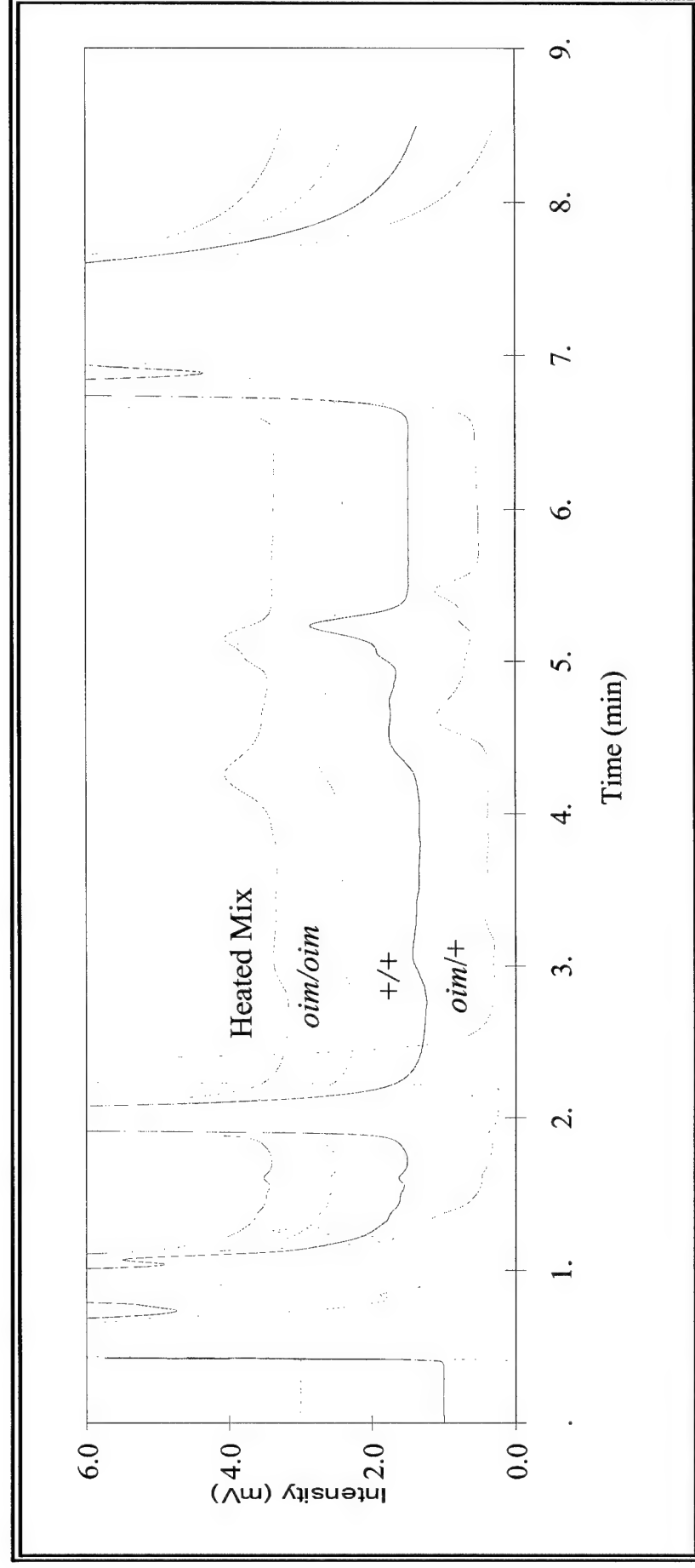
Figure 4D

oim/oim and +/+ Co-Elute
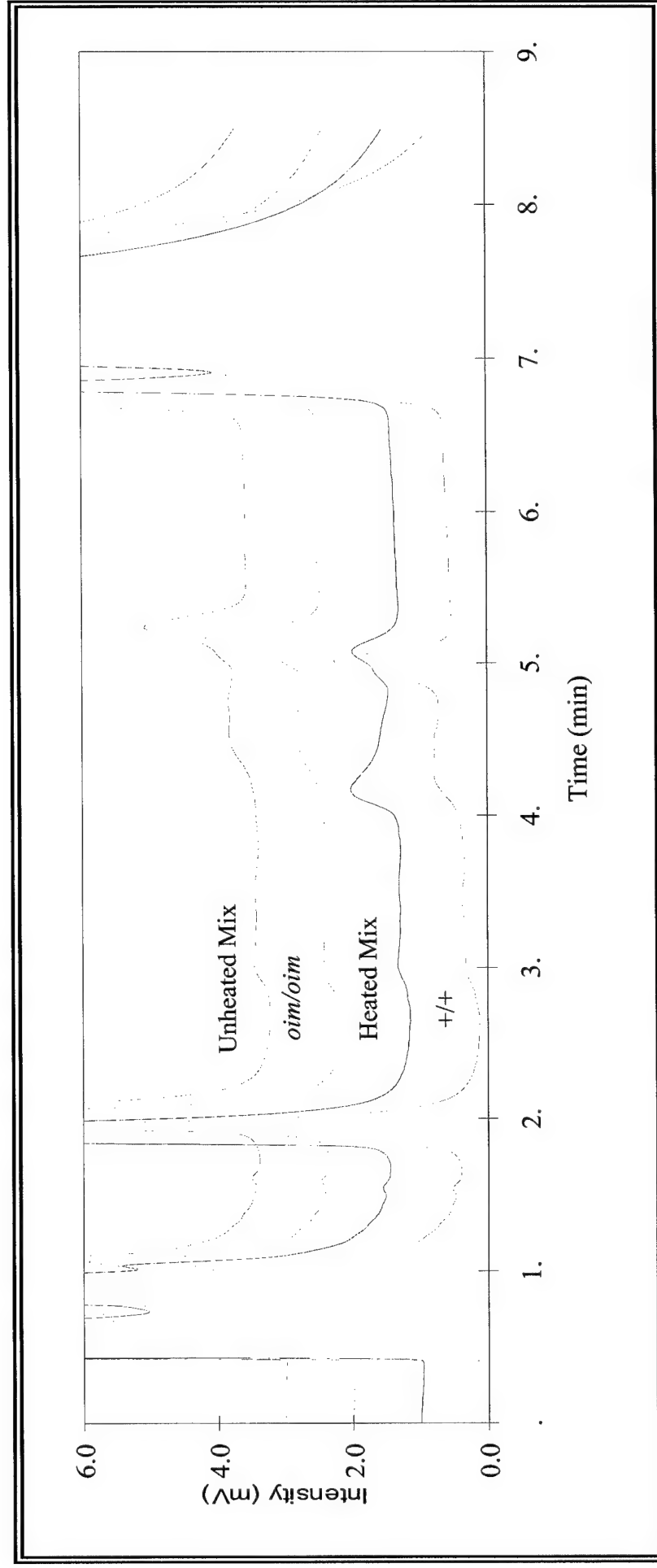
Figure 5A

Fas Melting Profile

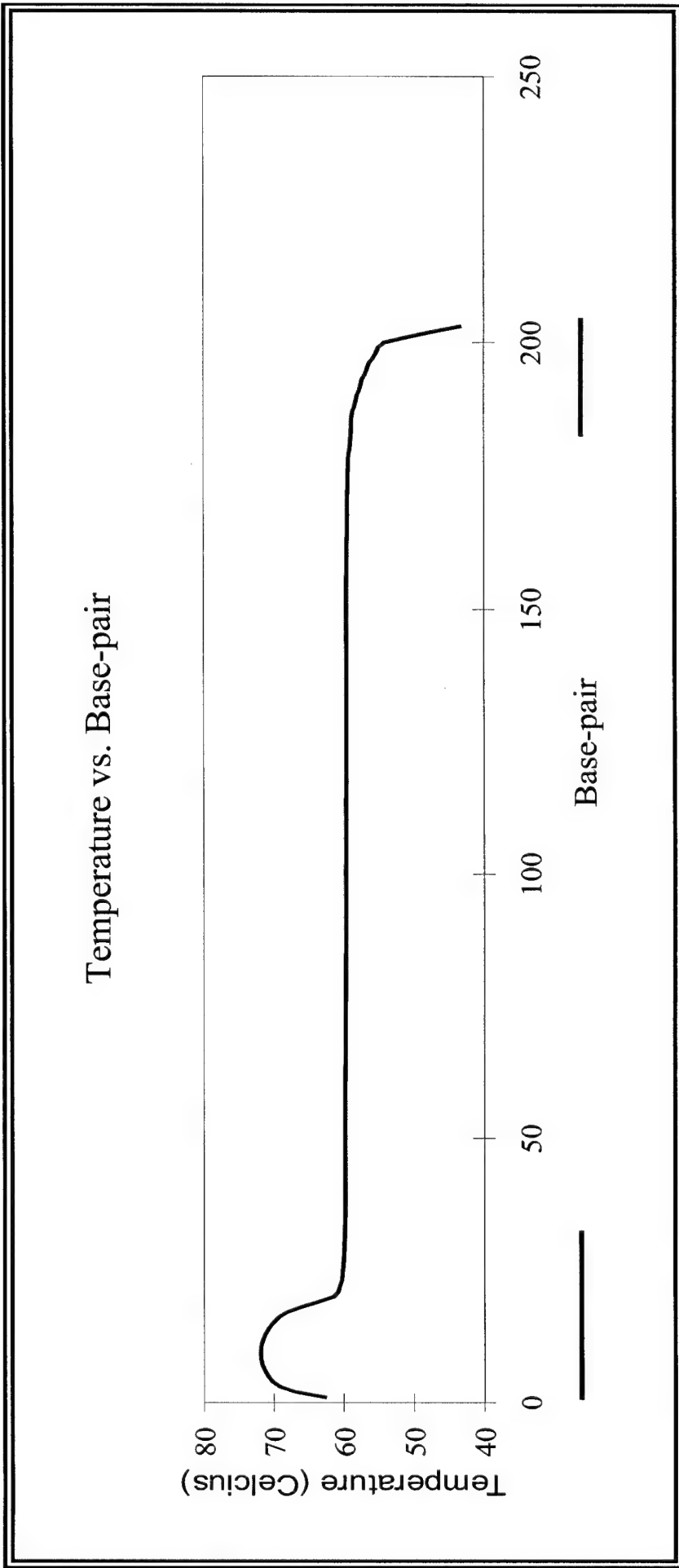Temperature vs. Base-pair

Base-pair

Figure 5B

Temperature and *Fas* Melting
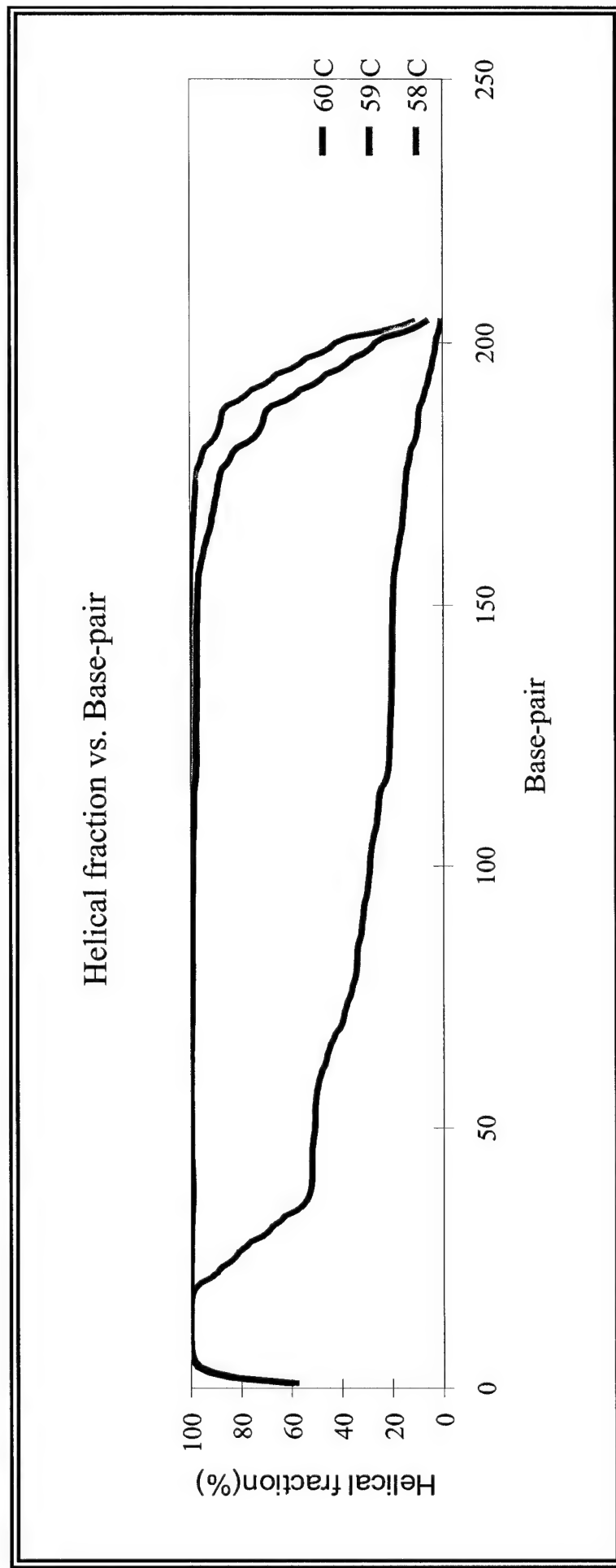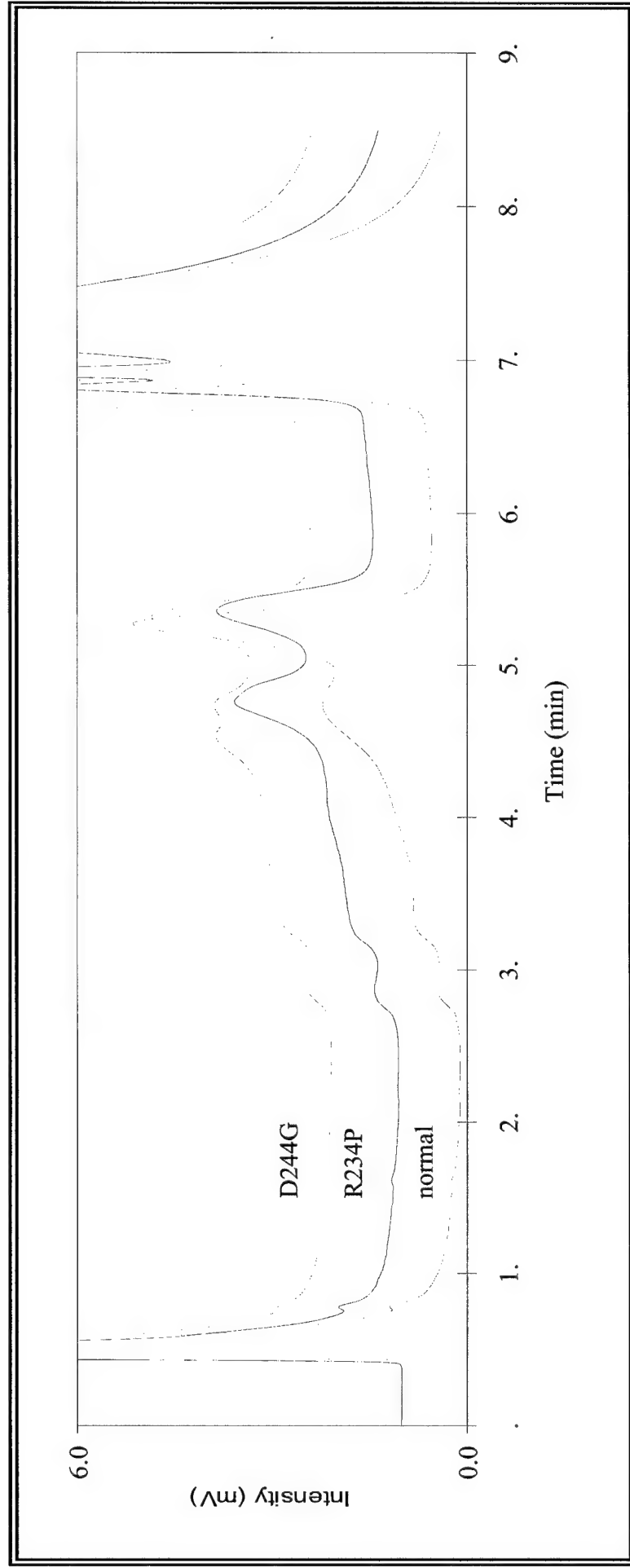
Helical fraction vs. Base-pair

Base-pair

Figure 5C

Fas Mutation Detection 59°C

SA119

Disease-causing Missense Mutations in the *PHEX* Gene Interfere with Cellular Trafficking of PHEX Protein. <u>Y. Sabbagh</u>,*[1] <u>G. Boileau</u>,*[2] <u>P. Crine</u>,*[2] <u>L. DesGroseillers</u>,*[2] <u>H. S. Tenenhouse</u>.[3] [1]Biology, McGill University, Montreal, PQ, Canada, [2]Biochemistry, Université de Montréal, PQ, Canada, [3]Biology, Pediatrics and Human Genetics, McGill University, Montreal, PQ, Canada.

Mutations in the *PHEX* gene are responsible for X-linked hypophosphatemia (XLH), the most prevalent form of inherited rickets in humans. The PHEX gene encodes a type II integral membrane glycoprotein with significant homology to the M13 family of metallopeptidases, which includes neutral endopeptidase 24.11 (NEP). We undertook to examine the effects of missense mutations on the cellular trafficking of PHEX protein. Four mutant PHEX cDNAs were generated by PCR mutagenesis: C85R, G579R, S711R, and E581V. The first three mutations were identified in patients with XLH. The fourth mutation, in the conserved catalytic domain (HEXXH), was examined in NEP and found to abolish catalytic activity but not to affect transport of the protein to the cell surface (Devault et al, J Biol Chem 263:4033, 1988). The cDNAs were sequenced to confirm that only the mutations specified above had been introduced. HEK 293 cells were transfected with the pcDNA3/RSV expression vector containing the wild type and mutant PHEX cDNAs and stable cell lines were established for each by selection of transfected cells with Geniticin. PHEX protein expression in crude membrane fractions was examined by western blotting using a monoclonal antibody generated against a human recombinant PHEX protein fragment (K_{121}-E_{294}). To assess whether expressed proteins were targeted to the plasma membrane, they were subjected to endoglycosidase digestion with PNGaseF and EndoH. The wild type protein, as well as the E581V mutant, were PNGaseF sensitive but EndoH resistant, suggesting that the proteins are fully glycosylated and expressed at the cell surface. Furthermore, biotinylation of cell surface proteins provided evidence for cell surface expression of the wild type and E581V proteins, in agreement with the endoglycosidase results. In contrast, mutants C85R, G579R and S711R, were PNGaseF and EndoH sensitive, indicating that the mutant proteins are not fully glycosylated and, therefore, retained intracellularly. In summary, we have shown that three *PHEX* missense mutations identified in XLH patients result in the synthesis of proteins that are not fully glycosylated. Our results suggest that the mutations result in misfolding of the nascent polypeptides and thereby interfere with the transport of the protein to the plasma membrane.

SA120

See Friday Plenary number F120.

SA121

See Friday Plenary number F121.

SA122

Bone Strength Variability in Mice Heterozygous for the *Cola2^oim* Mutation. <u>J. A. Wexler</u>,*[1] <u>R. Gupta</u>,*[2] <u>Y. Yershov</u>,*[2] <u>A. Kumar</u>,*[2] <u>R. D. Blank</u>.[1,2] [1]Endocrinology, Diabetes and Metabolism, Cornell University Medical Center, New York, NY, USA, [2]Division of Research, The Hospital for Special Surgery, New York, NY, USA.

Osteogenesis imperfecta (OI) is an inherited disorder of connective tissue caused by mutations of either the α1 or α2 procollagen genes resulting in qualitative or quantitative abnormalities in type I procollagen synthesis. Variation of disease severity among individuals with OI harboring the same collagen mutation has been described but is poorly understood. We previously mapped genes affecting bone strength and related traits in HcB/Dem recombinant congenic mice. We hypothesize that the segregation of background genes modifies the disease severity of OI and sought to test this by measuring biomechanical performance and supporting phenotypes in *Cola2^oim/+* mice. Mice were analyzed at 17 weeks of age. At sacrifice, animals were radiographed for evidence of fractures and image analysis, long bones were harvested and left humeri were subjected to 3-point bending. No spontaneous long bone fractures were observed in these mice. Selected phenotypes are summarized below.

Parameter	Males (N=119)	Females (N=106)	P-value
Mass (gm)	34.5 ± 4.9	26.0 ± 3.8	<0.001
Failure Load (N)	8.42 ± 1.46	7.05 ± 1.21	<0.001
AP OD (mm)	1.00 ± 0.08	0.91 ± 0.07	<0.001
AP ID (mm)	0.48 ± 0.07	0.43 ± 0.06	<0.001
ML OD (mm)	1.46 ± 0.10	1.36 ± 0.09	<0.001
ML ID (mm)	0.69 ± 0.92	0.66 ± 0.08	0.005
Stiffness (N/mm)	27.84 ± 6.11	23.21 ± 5.09	<0.001

We constructed a stepwise linear regression model for failure load as a function of the other directly measured traits with the equation: failure load = - 0.905 + 0.154 stiffness + 2.649 ML OD + 0.0325 mass. The ΔR^2 for stiffness is 0.615 (p<0.001), for ML OD is 0.0362 (p<0.001) and for mass is 0.0138 (p=0.003). This model demonstrates that 66% of failure load is determined by directly measured parameters. Sex was not an independent predictor of failure load.

Linkage mapping in the *Cola2^oim/+* mice is compared to our previous HcB/Dem data. This study demonstrates strong similarities to the HcB/Dem results with regard to both the mechanistic determinants of structural strength and to their genetic determination.

RD Blank is a stockholder of PE Biosystems.

SA123

See Friday Plenary number F123.

SA124

See Friday Plenary number F124.

SA125

Effects of Lower Leg Lengthening on Bone Mineral Density and Soft Tissue Composition of Legs in a Patient with Achondroplasia. <u>S. Takata</u>,* Ikata,* H. Yonezu.* Orthopedic Surgery, The University of Tokushima, Japan.

Achondroplasia is a common type of rhizomelic dwarfism, resulting in disproportion between the height of the trunk and that of extremities. In the present study, we applied dual energy X-ray absorptiometry (DXA) to measure bone mineral density, lean mass and fat mass of legs in a fifteen-year-old girl with achondroplasia to assess the effects of leg lengthening on bone mineral density and soft tissue composition of the legs.

Lower leg lengthening was performed on bilateral tibias by means of callus distraction (callotasis) using a unilateral dynamic external fixator. As for schedule of leg lengthening, the waiting period was 10 days, distraction period was 180 days at a rate of 1 mm/day, neutralization period was 84 days, and dynamic load period was 98 days. After dynamic load period, the external fixation was removed from the tibial shaft. As a result, overall treatment time was 372 days in this case, and the healing index was 42 days/cm.

The length of bilateral lower legs increased 9 cm, and consequently her height increased from 118 cm to 127 cm. L2-4BMD did not change after leg lengthening, whereas total body BMD decreased to 94.2% of the preoperative total body BMD. The BMD of the right leg and left leg decreased to 87.8% and 89.5% of the respective preoperative values. The lean mass of legs increased following leg lengthening, and the degree of increase of lean mass of leg was greater on the right side than on the left side. The fat mass of both legs increased following the procedure, and the degree of increase was greater on the left side than the right side. The results showed that lower leg lengthening induced an increase in fat and lean mass of the legs, whereas the BMD of bilateral legs decreased compared with the preoperative BMD.

SA126

See Friday Plenary number F126.

SA127

See Friday Plenary number F127.

SA128

Type II Autosomal Dominant Osteopetrosis (Albers Schönberg Disease) Results from an Infantile Resorption Defect. <u>O. D. Benichou</u>,*[1] <u>M. Brazier</u>,*[2] <u>C. Baudoin</u>,*[1] <u>M. de Vernejoul</u>.[1] [1]Unit 349, INSERM, Paris, France, [2]Biochimie Endocrinienne et Osseuse, CHU Groupe Hospitalier Sud, Amiens, France.

Type II autosomal dominant osteopetrosis (ADO II) is a rare inherited disease mainly characterized by a diffuse skeletal sclerosis which predominates in vertebral endplates, iliac wings, and skull base. Paradoxically, the main clinical manifestation is a strong predisposition to fractures. Although other forms of osteopetrosis have been clearly attributed to a bone resorption defect, the bone remodeling disturbance responsible for ADO II has not been proved so far.

We evaluated urinary hydroxylysylpyridinoline (urinary HP) by HPLC in 21 ADO II patients (17 adults and 4 children) and 46 normal matched controls. Six of the 21 ADO II adults (aged 22 to 71 years; mean 47.5) underwent lumbar spinal (L) and femoral neck (F) bone mineral densitometry at T0 and 2.8 to 4 years later (mean: 3.6 years). All available radiographs from these 21 subjects were reviewed.

Osteopetrotic adults had elevated levels of urinary HP (mean HP: 45±25) when compared to controls (mean HP: 30±16) (p=0.024) while osteopetrotic children had low levels of HP (mean HP: 108±39 unit) as compared to controls (mean HP: 182±55), indicating an infantile resorption defect (p<0.012).

Lumbar and femoral bone mineral density (BMD) respectively increased by 1.3 and 1.7% during the 3.6 years survey. This small increase was far from statistical significance (respectively p>0.89 and p>0.86), but could result from the short survey as compared to a lifetime. However, these slight variations of BMD were positive in 7 cases and negative in 4 cases, suggesting that BMD was overall stable during this period. We also compared radiographs of the whole skeleton in one patient at the age of 17 years and 33 years later. No modification of the bone sclerosis could be observed either in distribution or in intensity.

These biochemical, radiologic and densitometric data suggest that the pathogenic process responsible for ADO II involves a resorption defect that is active during skeletal growth, but most likely stabilizes spontaneously with adulthood. The mechanism of this stabilization is unknown but may involve an increased osteoclast recruitment since we and others previously found an elevated plasmatic TRAP activity in ADO II adults.

M110

Establishment and Functional Characterization of Kidney Cell Lines Derived from Osteosclerotic (oc/oc) Mutant Mice. S. Barale,*[1] M. Tauc,*[2] J. C. Scimeca,*[1] H. Parrinello,*[1] P. Hofman,*[3] P. Poujeol,*[2] G. F. Carle.*[1] [1]IAG – UMR 6549 CNRS, Université de Nice-Sophia Antipolis, Nice, France, [2]UMR 6548 CNRS, Université de Nice-Sophia Antipolis, Nice, France, [3]Service d'Anatomo-Pathologie, Hôpital Pasteur, Nice, France.

Osteosclerosis (oc) is an autosomal recessive lethal mutation which impairs bone resorption by osteoclasts, and induces a general increase of bone density in affected mice. We have recently shown that the gene encoding for the 116 kDa subunit of the vacuolar proton ATPase (V-ATPase) located on mouse chromosome 19, bears a 1.6 kb deletion in oc/oc mice between intron 1 and exon 3, and removes the translation start site of OC116.

V-ATPase is expressed in a polarized fashion in ruffled borders of osteoclasts and in the basal striations of proximal convoluted tubules (PCT). Ultrastructural examination of renal PCT of oc/oc mice exhibit abnormal basal striation as reported by Nakamura et al. (*FEBS Letters* 401 (1997) 207-212). In order to better characterize the effects of the oc mutation on V-ATPase function, we established PCT cell lines derived from kidneys of wild type and oc/oc mice. Functional tests based on proton transport are being used to test recombinant molecules of the MMUOC116 gene.

M111

Emergence of Fracture-resistant Cola2[oim/oim] Mice. N. P. Camacho,[1] E. A. McCarthy,*[2] S. Jain,*[1] R. Gupta,*[1] R. Wurzburger,*[1] C. L. Raggio,[1] R. D. Blank.[1] [1]Division of Research, The Hospital for Special Surgery, New York, NY, USA, [2]Neonatology, New York Cornell Hospital, New York, NY, USA.

There is significant intra-familial phenotypic variation among kindreds harboring type I collagen mutations, presenting as differences in the severity of osteogenesis imperfecta (OI). Although it is likely that segregation of loci other than the type I collagen genes contributes significantly to clinical presentation, the identity of these modifying loci remain unknown. The Cola2 [oim/oim] (oim/oim) mouse is a naturally occurring animal model of moderate-to-severe OI and has historically been maintained on an outbred B6C3 background. It therefore provides an ideal system for assessing the role of genes encoding proteins other than collagen on OI severity. The purpose of this study was to determine if inbreeding oim/oim mice would generate offspring displaying an attenuated phenotype. If so, these mice would provide a basis for genetic analysis to reveal modifying loci.

Heterozygous oim/± breeder mice obtained from the Jackson Laboratory (Bar Harbor, ME) produced litters of 6-10 mice, which segregated at the Cola2 locus at the expected 1:2:1 ratio. Mice shown to be Cola2 [oim/oim] were subjected to 5-6 subsequent generations of brother-sister mating. By generation N6 and N7, the bone properties of these partially inbred (IB) oim/oim mice (n=22) were compared to those of oim/oim offspring (N1) (n=19) obtained from original Jackson Lab breeders and their N1 offspring at 14 weeks of age. The comparision indicates that the IB seem to have modifying genes which allow for increased bone strength and decreased fracture rate:

	N1	IB	p
Fractures	3.2 ±1.6	1 ±1.1	<0.001
Weight	25.3 ±1.2	23.7 ±2.1	0.004
Length	15.25 ±0.37	15.59 ±0.69	NS
AP Outer Diam.	1.49 ± 0.20	1.61 ±0.19	NS
ML Outer Diam.	1.15 ±0.11	1.27 ±0.17	0.018
Density$_{metaphyseal}$	1.02 ±0.33	1.57 ±0.58	0.002

The stresses associated with breeding therefore appear to be sufficient to serve as the selective pressure for bone strength genes in this system. Genotypes of the IB mice are related to the locations of bone strength loci previously mapped in HcB/Dem recombinant congenic mice.

M112

Bone Mineral Content is an Important Contributing Factor in the Maintenance of an Intact Vertebral Shape in Children with Osteogenesis Imperfecta. D. Kok,*[1] A. Kerssen,*[1] C. S. P. Uiterwaal,*[2] A. J. VanDongen,*[3] P. P. G. Kramer,*[4] R. H. H. Engelbert,*[5] H. E. H. Pruijs,*[1] D. H. Schweitzer,[6] R. J. B. Sakkers.*[1] [1]Pediatric Orthopedics, UMCU-WKZ, Utrecht, Netherlands, [2]Epidemiology, UMCU-WKZ, Utrecht, Netherlands, [3]Nuclear Medicine, UMCU, Utrecht, Netherlands, [4]Radiology, UMCU-WKZ, Utrecht, Netherlands, [5]Pediatric Physiotherapy, UMCU-WKZ, Utrecht, Netherlands, [6]Endocrinology, Reinier de Graaf Groep, The Hague, Netherlands.

Osteogenesis imperfecta is a heterogeneous disorder of collagen with multiple phenotypic expressions. In a previous study, our group has shown clear correlations between DXA outcomes at the lumbar spine and the os calcis and functional capabilities of the individual children. The current study aims to analyze possible relationships between DXA outcomes and vertebral deformities in these children. Fifty one children (25 boys and 26 girls, mean age 10.5 (SD 4.2) and 11.0 (SD 3.5), respectively) with osteogenesis imperfecta were studied in a cross-sectional design. Excluded were all children either with previous or with current use of bisphosphonates and with missing values for either DXA of the lumbar spine or the os calcis. A DXA measurement of the lumbar spine (L1-L4) was made as well as a DXA of the os calcis at both sides and the mean value of these calcaneal DXA's was calculated. X-rays were made of the spine. Vertebral geometry, defined by the anterior/posterior (A/P) and mid/posterior (M/P) vertebral body height ratio's, was manually measured (L1-L4). After calculating the mean of A/P and M/P ratio's of the lumbar vertebrae L1-L4, a wedge deformation was defined as an AP ratio of less than 0.8 or more than 1.2. Biconcavity was defined as an MP ratio of less than 0.8. Multiple regression analyses were performed between DXA outcomes, age and the two main geometrical types of vertebrae (type 1: normal shape (25 patients) and type 2: either wedge or biconcave shape (26 patients)). The results are shown in the table.

		Lumbar spine (L1 - L4)		Calcaneus	
		BMC (g/cm)	BMD (g/cm2)	BMC (g/cm)	BMD (g/cm2)
Mean group difference	Unadjusted	-2.9 (2,7)	-0.12 (0.05)*	-0.6 (0.7)	-0.06 (0.04)
	Age adjusted	-6.4 (2.3)**	-0.17 (0.05)***	-1.2 (0.6)*	-0.08 (0.04)*

Mean group differences (SEM) are obtained by subtracting the mean value of those with deformed vertebrae (n=26) from the mean value of those without deformed vertebrae (n=25). * = p < 0.05, ** = p <0.01, *** = p < 0.0001

In conclusion, in children with medically untreated osteogenesis imperfecta, a positive correlation is seen between bone mineral content and the vertebral geometry, but only after adjustment for age. The results clearly indicate the importance of the quantity of mineralized bone in the geometrical preservation of vertebrae in osteogenesis imperfecta. Increasing the quantity of mineralized bone with medical treatment may therefore alter the natural course of the disease. For this reason, clinical randomized prospective trials with bisphosphonates are currently conducted.

M113

Gain in BMD And Grip Strength after One Year of Pamidronate Treatment in 132 Children with Osteogenesis Imperfecta. H. Plotkin, K. Montpetit,* S. Cloutier,* N. Bilodeau,* N. Gervais,* M. Rabzel,* R. Travers, F. H. Glorieux. Genetics, Shriners Hospital for Children, Montreal, PQ, Canada.

Osteogenesis imperfecta (OI) is a rare disease characterized by osteopenia and bone fragility. Bisphosphonates has proven to be effective to increase bone density, decrease pain and decrease the number of fractures in children with OI. We present here the results of the changes in bone mineral density (BMD) measured by DXA (Hologic 4500A) and bilateral grip strength (GS) measured with a hand dynamometer (average of three consecutive measurements, expressed as Z-score for age) in a group of patients with OI treated with pamidronate IV for one year. Age at start ranged from 0.1 to 21 years of age (mean 7.7 ± 4.9). Nineteen patiens had type I OI, 30 type III, 41 type IV, 9 type V and 33 patients could not be classified as per the Sillence classification. Patients received pamidronate at a dose of 3 mg/kg/cycle every 4 months (>3 years of age), or 1.5 mg/kg/cycle every 2 months (<3 years of age).

BMD Z-score increased from -5.2 ± 1.4 to -3.6 ± 1.4 (n=132) and GS Z-score of the dominant side increased from -2.60 ± 1.07 to -2.15 ± 1.25 (p<0.01) in the patients as a group (n=50). Grip strength was low at baseline in all subjects, and increased with treatment in all. Progress was faster than in normal subjects for the milder forms.

Type	n	BMD Z start	BMD Z 12 mo.	N	GS Z Start◆	GS Z 12 mo◆
I	19	-4.1 ± 0.8	-2.8 ± 0.6*	11	-2.19 ± 0.7	-1.15 +0.8*
III	30	-6.1 ± 1.2	-4.3 ± 1.3*	8	-3.30 ± 0.8	-3.14 ± 0.5
IV	41	-5.3 ± 1.2	-3.5 ± 1.2*	20	-2.57 ± 1.1	-1.97 ± 1.3*
V	9	-4.9 ± 1.3	-3.4 ± 1.3*	5	-2.87 ± 0.7	-2.78 ± 0.7
?	33	-5.3 ± 1.6	-3.8 ± 1.8*	6	-2.18 ± 1.6	-1.59 ± 0.9

◆ dominant side *p<0.05

In this larger group of patients, gain in BMD (Z-score) was similar to the one observed in a first cohort of 30 patients (-5.3 to -3.4).

Muscle force as assessed by grip strength increased in children with all types OI. This quantifies the positive clinical effects of the treatment. Whether these results are directly related to the drug effect or are rather the consequence of the decrease in pain experienced by all subjects, remains to be evaluated.

Use of Representational Difference Analysis to Identify Candidate RFLPs Linked to Modifiers of the Murine Cola2oim/oim Osteogenesis Imperfecta Phenotype

A. N. Patani,[*1] A. Pincavage,[*2] J. Bankston,[*2] N. P. Camacho,[2] R. D. Blank.[1]
1.   Endocrinology/Medicine, University of Wisconsin, Madison, WI, USA, 2.   Research Division, Hospital for Special Surgery, New York, NY, USA.

The *Cola2$^{oim/oim}$* mouse harbors a nonsense mutation in the gene encoding the $\alpha 2$ chain of type I collagen and consequently produces type I collagen composed of $\alpha 1$ homotrimers rather than $(\alpha 1)_2(\alpha 2)$ heterotrimers. This mutation is maintained on an outbred B6C3 background, but we have noted that inbreeding results in attenuation of the bone fragility phenotype that is characteristic of *oim/oim* mice. The outbred animals averaged 3.2 ± 1.6 long bone fractures each under normal cage activity while the partially inbred animals averaged 1.0 ± 1.1 long bone fractures. In an attempt to identify loci whose segregation modifies the *oim/oim* phenotype, we used pools of genomic DNA prepared from outbred and partially inbred *oim/oim* animals to perform representational difference analysis. This PCR-assisted subtraction method results in preferential amplification of restriction fragments present exclusively in one of the two DNA sources. We amplified representative populations of BamH1 restriction fragments from the outbred and inbred DNA pools by PCR to generate "amplicons." We iteratively subtracted outbred from inbred amplicons and amplified the difference products. Following 3 rounds of subtraction and amplification, difference products were cloned into a plasmid vector and analyzed. Unique, polymorphic clones obtained by this method are putative markers for genes that modify the *oim/oim* phenotype. Representational difference analysis provides a complementary approach to linkage mapping in localizing genes of interest.

Geometry as a Heritable Determinant of Bone Strength. D.H.Goddard[1,2], C. Goddard[2], J. Hect[4], E. Kim[3], E.R. Myers[3], R. D. Blank[3] and R.S. Bockman[3]. [1]New York Methodist Hospital, & [2]Arthritis and Osteoporosis Center, Brooklyn, NY, [3]Hospital for Special Surgery, NY, NY, [4]HAFTR High School, Lawrence, NY

Fracture susceptibility is determined by a combination of genetic and environmental factors, which act in concert to establish whole bone strength. Whole bone strength depends on the mineral and organic content as well as geometry and the integrity of the structural components of the bone. Recent studies have focused on bone geometry as a potential predictor of fracture risk in specific family groups with high fracture susceptibility. Hypothesizing that individuals with similar volumetric bone mineral densities (vBMD) might differ markedly with regard to bone geometry, we used peripheral QCT scans of the forearm to measure vBMD, bone diameters, and to calculate the axial moments of inertia (I) in a 3-generation family. Typical scans of the radius using a Stratec XCT-2000, peripheral QCT are shown for the 68 year old father, the 67 year old mother and the 45 year old daughter in the figure below.

Father

Mother

Daughter

	vBMD (mg/cc)	I
father	1140	1379
mother	1225	628
daughter	1215	356
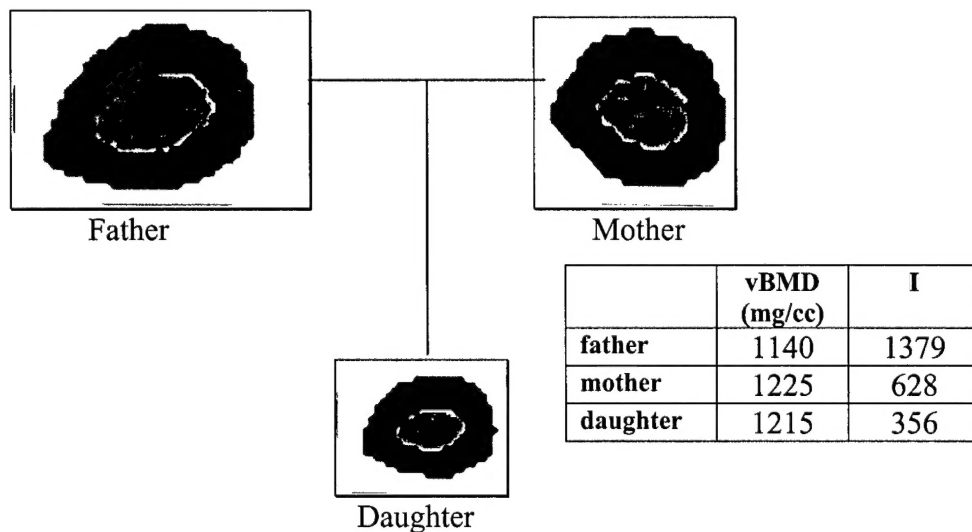
While mother and daughter have similar vBMDs, they display considerable differences in the cortical diameters. This results in large differences in the calculated axial moment of Inertia. It is not possible to determine the contribution of aging to the mother-daughter difference in bone size from these data alone. A striking sexually dimorphic difference was observed in the I values for the father and mother. All members of this family have low BMD values, however, it is the striking difference in bone size that highlights the potential importance of geometry as a determinant of bone strength and in evaluating fracture susceptibility.